International Journal of Multiphase Flow 35 (2009) 1100–1118

Contents lists available at ScienceDirect

International Journal of Multiphase Flow

journal homepage: www.elsevier.com/locate/ijmulflow

Jump conditions for filtered quantities at an under-resolved discontinuous interface. Part 1: Theoretical development

A. Toutant [a,b,c,*], M. Chandesris [a], D. Jamet [a], O. Lebaigue [a]

[a] CEA, DEN, DER/SSTH/LMDL, F-38054 Grenoble, France
[b] PROMES-CNRS, UPR 8521, Perpignan, France
[c] Université de Perpignan Via Domitia, France

ARTICLE INFO

Article history:
Received 28 November 2008
Received in revised form 29 May 2009
Accepted 22 July 2009
Available online 23 August 2009

Keywords:
Two-phase flow
Jump conditions
Matched asymptotic expansions
Filter
Surface tension
Turbulence
DNS
LES
Scale similarity hypothesis
Curvature

ABSTRACT

In this paper, we study turbulent two-phase flow. We consider the level of description where only the large scales of turbulence and the large deformations of bubbles are explicitly described:

- the small scale of turbulence are not represented and we are close to the Large Eddy Simulation concept,
- the mean geometry of each bubble is explicitly described but the small deformations of the bubbles are not represented. The bubble interface is still supposed to be infinitely thin (*i.e.* interfaces are supposed to be under-resolved and discontinuous).

At this level of description, there is no reason that the well known jump conditions are still valid. Using a two-step methodology, we determine the jump conditions for filtered quantities (*i.e.* local mean velocity and pressure) at the under-resolved discontinuous interface (*i.e.* small deformations of the interface are not represented). In particular, we express the velocity of the under-resolved discontinuous interface as a function of the filtered velocity, a scale similarity hypothesis and the time evolution of the interface mean curvature.

1. Introduction

Many industrial and environmental applications (*e.g.* convective boiling, spray formation and direct contact heat exchanger) involve high Reynolds number turbulent multiphase flows. Because nonlinear effects mainly drive the behavior of such flows, Direct Numerical Simulation (DNS) have to entail a number of degrees of freedom proportional to the third power of the Reynolds number. This extremely hard constraint makes it impossible to use DNS for industrial applications.

Until now, the large majority of numerical computations have adopted Reynolds Averaged Navier-Stokes (RANS) modeling. Classical single-phase turbulence models have been implemented in one or in both phases without direct consideration of the influence of the multiphase topology of the flow on the turbulence behavior. For example, Sato and Sekoguchi Sato and Sekoguchi (1975) derived a mixing length model based on a void fraction consideration for bubbly channel flows, by splitting the turbulence into shear and multiphase induced turbulence. Some interesting comparisons between classical RANS modeling for two-phase flows have been reported for instance in (Homescu and Panday, 1999) for condensation on a horizontal tube.

Large Eddy Simulation (LES) has also been used for multiphase flow computations. A large amount of these works deals with particles laden flows or sprays, involving particles even smaller than the Kolmogorov scale (see for instance Boivin et al., 2000; Eaton and Fessler, 1994; Elghobashi et al., 1984; Lain et al., 2002; Menon et al., 1996; Squires and Yamazaki, 1995). Another scope studied extensively is the case of non-deformable shear-free surface of an open channel flow. See, *e.g.*, the description of the near shear-free surface turbulence that Calmet and Magnaudet Calmet and Magnaudet (2003) deduced from their LES and the subgrid scales modeling of Shen and Yue Shen and Yue (2001). Regarding the modeling of wave breaking, Christensen and Deigaard Christensen and Deigaard (2001) and Watanabe and Saeki Watanabe and Saeki (2002) adopted a standard LES model coupled with a Volume of Fluid (VOF) free surface approach. Moreover, Lakehal *et al.* Lakehal et al. (2002) derived a subgrid scale model based on the analytical analysis of Drew and Lahey Drew and Lahey (1987) on the forces acting on a sphere and on the scale similarity principle of Bardina *et al.* Bardina et al. (1983). All these contributions aim at finding a two-phase equivalent to the single-phase LES concept. However,

* Corresponding author. Address: CEA, DEN, DER/SSTH/LMDL, F-38054 Grenoble, France.
E-mail address: adrien.toutant@univ-perp.fr (A. Toutant).

0301-9322/$ - see front matter © 2009 Elsevier Ltd. All rights reserved.
doi:10.1016/j.ijmultiphaseflow.2009.07.009

from a modeling point of view, the two-phase LES concept has not been defined. This paper is an attempt to define rigorously this concept at a given level of description.

We name this two-phase LES concept at a given level of description Interfaces and Subgrid Scales (ISS). It consists in solving the two-phase flow features at the grid scale of the numerical method and to take into account the unresolved scales with subgrid models. In this regard, the concept is strictly identical to the single-phase LES concept. However, in the present paper, we restrict the model in that the filter is much smaller than the bubbles. With this restriction, fully deformable interfaces that remain much larger than the filter size and much larger than the turbulence scales are captured in a DNS-like approach while the smallest scales of turbulence within each phase and the interface smallest deformations have an unresolved scale part that is modeled. The choice of this level of description could be surprising. Actually, it is very convenient for the applications of interest in the nuclear industry. Indeed, in a typical sub-channel situation (*e.g.*, 15 MPa and water flow in a PWR sub-channel), the Reynolds number using the mean velocity is equal to 300,000, the turbulent Reynolds number using the friction velocity is close to 11,800 and the Kolmogorov scale is 1 μm whereas the typical bubble size is supposed to be close to 150 μm. Therefore, the use of a simple subgrid model between 1 and 10 μm allows a drastic reduction of the number of nodes in the space discretization (division by 1000 in 3D). In practice, we plan that the ISS simulations will be realized with the same numerical tool that we use for DNS: a "sharp-interface" version of the Front-Tracking approach. This original method allows in particular a sharp pressure jump corresponding to the surface tension without numerical parasitic currents (Mathieu, 2003). Although a detailed presentation of the implementation of ISS is behind the scope of this paper (numerical instabilities are difficult to foresee), the ISS jump conditions can be directly integrated to the actual numerical algorithm. The corresponding jumps are simply new interfacial terms added to the capillary forces.

Obviously, the chosen level of description implies that far from the interface classical single-phase LES model could be used. The challenge consists in finding the jump conditions for the filtered quantities at the under-resolved discontinuous interface. These jump conditions have to correctly account for the interfacial transfers at the under-resolved discontinuous interface. To our knowledge, this paper is the first attempt to define mathematically a discontinuous under-resolved interface and to propose the corresponding jump conditions.

The present article is organized as follows. Section 2 describes the main ideas of our two-step methodology for defining the ISS concept: first, we apply a centered filter that smears the interface and, second, we determine the discontinuous problem equivalent to the filtered one. Section 3 deals with the first up-scaling step of the approach. In particular, we exhibit the subgrid terms specific to two-phase flows, sort them out and model the preponderant contributions. Section 4 focuses on the second up-scaling step. The matched asymptotic expansions are used to determine the jump conditions for the filtered quantities at the discontinuous under-resolved interface. In particular, we define the velocity of the discontinuous under-resolved interface with the filtered velocity of the phase and the time evolution of its principal curvature radius.

2. A two-step methodology

Generally, the formalism of LES uses a filter defined as a product of convolution. In order to have properties like commutation with derivation, it is necessary for the convolution kernel to be independent of time and space (Sagaut, 2003). However, while applying this filter on flows with discontinuities like flames, shocks or interfaces, the jump related to the discontinuity contributes to the subgrid fluctuations. This is an important issue because classical subgrid scale models are founded on the assumption that the subgrid fluctuations originate from turbulence only. Consequently, they are unable to model the part of the subgrid fluctuations due to the contribution of the discontinuity. Sagaut and Germano Sagaut and Germano (2005) have exhibited this paradigm. In order to use classical LES models in agreement with their original assumptions, these authors recommend to use non-centered filters and show how to adapt LES models to these filters. In this way, the interface is not smeared out because, by construction of the filter, no control volume ever contains the interface. However, the use of non-centered filters does not allow to define a filtered interface because the geometry is never filtered. This approach implicitly assumes that the interface smallest deformations are bigger than the filter. Consequently, this concept is restricted to perfectly resolved interface: the velocity field is filtered but not the interface. This occurs only if the interface is enough tight (*i.e.* there is no coupling between the small vortex of the phases and the interface deformations). In this case, it is quite natural to use classical single-phase LES model and specific jump conditions are not necessary.

However, we are not in this case and we are precisely interested in the coupling between the smallest coherent turbulence structures and the interface deformations. This implies that if a part of the velocity field is not viewed by an observer because it has been filtered, this same observer should not see all the interface but only the under-resolved part of the interface geometry (see the illustration Fig. 1). Thus, we have to define the under-resolved interface and to find the jump conditions that take into account, at this scale of description, the subgrid transfers that originate from the turbulence and interface coupling in the interfacial region.

In order to find the jump conditions for the filtered quantities at the under-resolved interface, we propose to follow a two-step up-scaling methodology. First, we apply a centered filter to the equations governing the problem at the DNS scale. Since this filter is always centered, it can be crossed by the interface and the discontinuous interface becomes a continuous transition zone. In this way, the interface geometry is filtered just as the velocity field and specific subgrid terms are expected to be related to the presence of the interface. However, the nature of the interface geometry changes and it is difficult to compare the obtained continuous transition zone to the original discontinuity. Furthermore, this continuous vision of interfaces corresponds to a description level where the coupling between the two phases is difficult to capture numerically. More precisely, there are two numerical issues at this description level. The first one consists in avoiding numerical diffusion of the profile in order to keep constant the size of the transition zone. The second one concerns the numerical cost necessary to capture these profiles. Because filtered quantities evolve very strongly within the transition zone, the mesh size required to capture these strong variations would be much smaller than the filter size, which is in contradiction with the LES concept. On the contrary, a discontinuous formalism would tackle these two issues.

Thus, we have to perform a second up-scaling step to go from this continuous description of the interface to a new discontinuous description of the interface, *i.e.* the description level of the proposed ISS concept. At this latter level, the observer cannot see the detail of the transition zone, he can only see it as a discontinuity where jump conditions, that take into account the coupling between the phases, are applied. One of the major modeling issues is then to determine these jump conditions.

Before going further, we summarize the three description levels that we have just introduced: (Fig. 1).

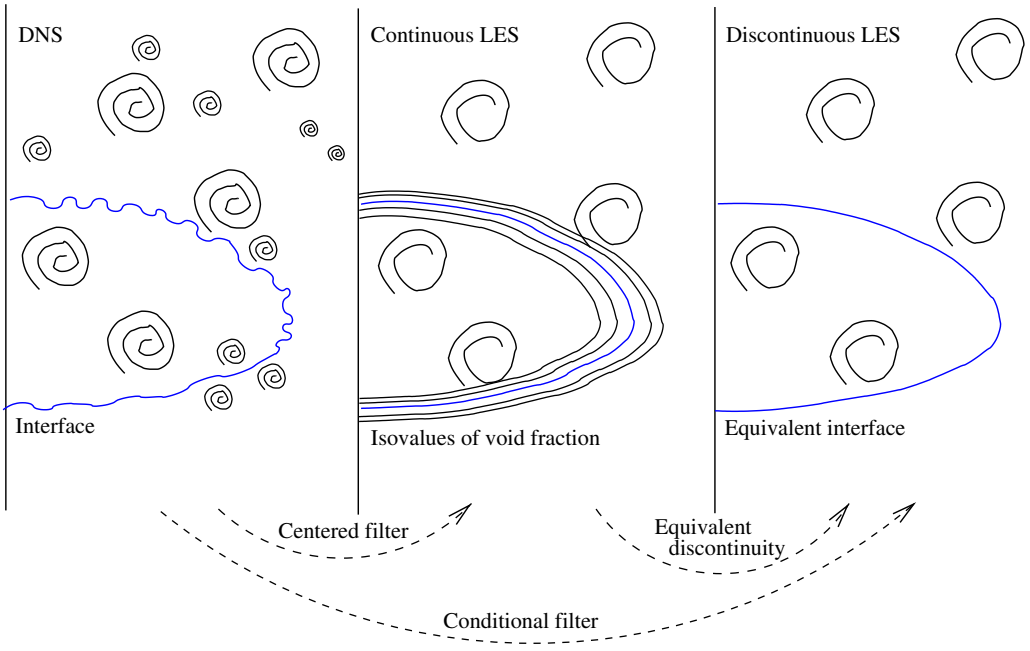

Fig. 1. A two-step methodology. Schematic representation of resolved coherent turbulence structures and interface in the case of a DNS, a continuous LES and a discontinuous LES, respectively.

- At the DNS level, all scales of the interfaces and of the velocity fields are accurately described. Thus, the Navier-Stokes equations are valid without adding any subgrid models. At this level, interfaces are viewed as discontinuity surfaces.
- At the continuous LES level, only large scales of both turbulence and interfaces are represented. Specific subgrid models take into account the effect of the subgrid fluctuations (due to turbulence and the presence of a discontinuity) on the filtered velocity and on the filtered interface. At this level, interfaces are viewed as continuous transition zones. They have a finite non-zero thickness.
- At the discontinuous LES level or the ISS level, only large scales of both turbulence and interfaces are represented. At this level, interfaces are again considered as surfaces of discontinuity. They are infinitely thin. The interfacial transfers at this new discontinuous interface are taken into account through appropriate jump conditions.

It can be noticed that a similar two-step up-scaling methodology with three levels of description is used with success by Chandesris and Jamet Chandesris and Jamet (2006), Chandesris and Jamet (2007) to study transport phenomena at a fluid/porous interface. A filter is applied to the DNS equation all over the domain (including the interface between free and porous media). Thus, the fluid/porous interface becomes a continuous transition region. The interfacial transfers are modeled at this continuous level of description. Then, a second up-scaling step is performed to obtain a discontinuous equivalent problem that takes into account the interfacial transfers *via* appropriate jump conditions. Reasoning by analogy with these studies of the fluid/porous interface, we can rename the description levels introduced:

- DNS corresponds to the microscopic level of description,
- continuous LES corresponds to the mesoscopic level of description,
- discontinuous LES or ISS corresponds to the macroscopic level of description.

2.1. First up-scaling step: centered filtering operation

To go from the microscopic level of description to the mesoscopic level of description, we apply a spatial centered filter to the equations governing the problem at the microscopic scale. Applying a spatial filter across the discontinuity, we transform it into a continuous transition zone. As shown in Section 3, this operation makes appear specific subgrid terms related to the correlations between the interface and the velocity field. Thus, specific models need to be developed to take into account the non-turbulent parts of the subgrid terms that proceeds from the presence of the discontinuity. This is why it is improper to speak about LES in our case. Indeed, the aim of both ISS and LES consists in modeling subgrid fluctuations but, in the ISS concept, fluctuations are not only due to turbulence. They are also due to the presence of the discontinuity. It can be noticed that the non-turbulent parts of the subgrid terms also exist in laminar and in 2D flows. For these two types of flows, there is no stretching phenomenon of coherent structures that get involved in the energy cascade and they are thus not turbulent. In the ISS concept, non-turbulent parts of the subgrid terms exist and have to be modeled properly.

2.2. Second up-scaling step: stiffening of the transition zone

In this second up-scaling step, we go from the mesoscopic level of description to the macroscopic level of description. The difficulty lies in the specification of the jump conditions at the under-resolved interface that are such that the macroscopic problem is indeed equivalent to the mesoscopic one, *i.e.* so that the solutions of the two problems are identical outside of the interfacial transition region. This particular up-scaling problem has been thoroughly studied for liquid/liquid, liquid/vapor or liquid/solid interfaces (*e.g.* Emmerich, 2003; Anderson et al., 2001) and can be referred to as finding the sharp-interface limit of a diffuse interface model. Different approaches can be used to perform this up-scaling (*e.g.*) the surface-excess theory of interfacial transport processes (Edwards et al., 1991), the method of matched asymptotic expansions (Zwillinger, 1989). These methods can be very different in their

respective technical steps, however, they are based on the same main idea. By construction, the macroscopic model is not suited to describe the problem in the interfacial transition region. Indeed, it is based on closures that are valid far from the interface but not in the interfacial transition region. Thus, compared to the mesoscopic model, some physical features are not or not correctly accounted for by the macroscopic model in the interfacial transition region. The idea is thus to assign the amount of the quantity ϕ that is not seen by the macroscopic model compared to the mesoscopic model to the interface such that the macroscopic model is indeed equivalent to the mesoscopic one. This is done by means of surface-excess quantities that are assigned to the interface. As a consequence, these surface-excess quantities appear in the jump conditions at this interface.

We recall that for any physical field ϕ, its excess quantity is defined by:

$$\phi^{ex} \triangleq \int_{-\infty}^{+\infty} \bar{\phi}(\xi_3) - \tilde{\phi}(\xi_3) d\xi_3 \tag{1}$$

where $\bar{\phi}$ is the mesoscopic representation of the studied field, $\tilde{\phi}$ is the macroscopic representation of this field and ξ_3 is the coordinate normal to the interface (see Appendix A for the definition of the local coordinates associated to the interface). This definition is illustrated in Fig. 2 where the excess quantity is represented by the shaded area. It represents exactly the amount of the ϕ field that is not seen by the macroscopic model in the interfacial transition region compared to the mesoscopic model.

The surface-excess theory (Edwards et al., 1991) is more generic and easy to implement than the method of the matched asymptotic expansions. However, it does not provide closed expressions for the jump conditions when the problem is non-linear, which is our case. Since we are looking for closed jump conditions at the macroscopic scale, we use in this paper the method of the matched asymptotic expansions to perform this second up-scaling.

Using this two-step strategy, we are able to derive the jump conditions that the filtered quantities must satisfy at the discontinuous under-resolved interface. We show in particular that these jump conditions are the same as those satisfied by microscopic quantities except that additional terms appear. These additional terms take into account the unresolved part of the velocity fields, the interface geometry and their coupling. Moreover, the location of the discontinuous under-resolved interface where these jump conditions must be satisfied is predicted by an original transport equation. The modeling of this transport equation is a major result of this paper. Indeed, we show that the speed of displacement of the discontinuous under-resolved interface is not trivial and is not only equal to the fluid velocity at the interface, as it is the case at the microscopic scale.

3. Continuous LES

In this section devoted to the first up-scaling step of our strategy, we present the filtered equations and the specific subgrid terms. They have already been exhibited in (Toutant et al., 2006; Toutant et al., 2008; Labourasse et al., 2007), but we remind the results here for the sake of completeness.

3.1. DNS equations

In each phase, the flow is supposed to be incompressible and isothermal. The mathematical formalism we use is the so-called one-fluid formulation (Delhaye, 1974; Ishii, 1975). In this formalism, any physical variable, ϕ, is defined by $\phi = \sum_k \chi_k \phi_k$ where χ_k is the phase indicator function ($\chi_k = 1$ in phase k and 0 elsewhere). Using this formalism, three equations allow to describe the flow:

- the incompressibility constraint,
- the transport equation of the phase indicator function,
- the momentum equation.

They are respectively given by:

$$\nabla \cdot \mathbf{u} = 0 \tag{2a}$$

$$\frac{\partial \chi_k}{\partial t} = -\mathbf{u} \cdot \nabla \chi_k \tag{2b}$$

$$\frac{\partial \rho \mathbf{u}}{\partial t} + \nabla \cdot (\rho \mathbf{u} \otimes \mathbf{u}) = -\nabla p + \rho \mathbf{g} + \sigma \kappa \mathbf{n} \delta_\sigma + \nabla \cdot (\mu(\nabla \mathbf{u} + \nabla^T \mathbf{u})) \tag{2c}$$

with

$$\nabla \chi_k = -\mathbf{n}_k \delta_\sigma \tag{3}$$

where t is the time, $\mathbf{u}$ the velocity, p the pressure, ρ the density, μ the dynamic viscosity, $\mathbf{n} = \mathbf{n}_g$ the unit normal to the interface (from gas to liquid), $\kappa = -\nabla_s \cdot \mathbf{n}$ the interface curvature ($\nabla_s \cdot$ is the surface divergence operator), σ the surface tension, which is assumed constant in this paper and δ_σ the Dirac function indicating the interface. The system (2) is valid on the entire domain in the sense of distributions.

3.2. Filtered equations

Let us note $\bar{\cdot}$ the volume filtering operation defined by:

$$\bar{\phi}(x^0) = \int_{\mathbb{R}^3} G(x^0 - x)\, \phi(x)\, dx \tag{4a}$$

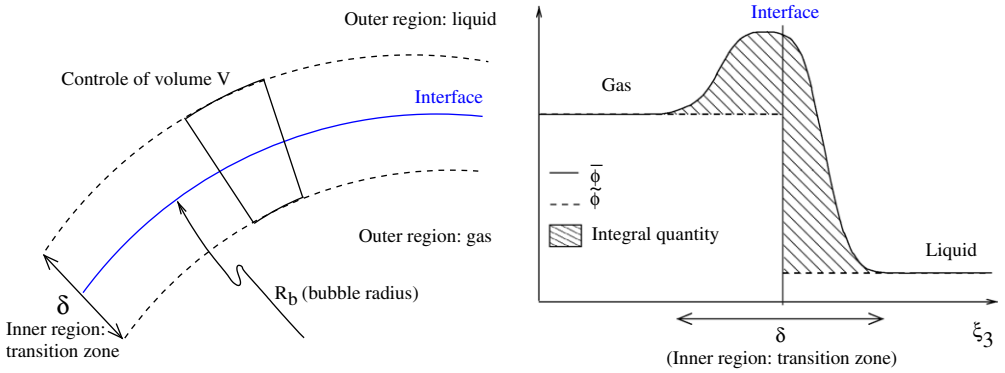

Fig. 2. Illustration of a surface-excess quantity.

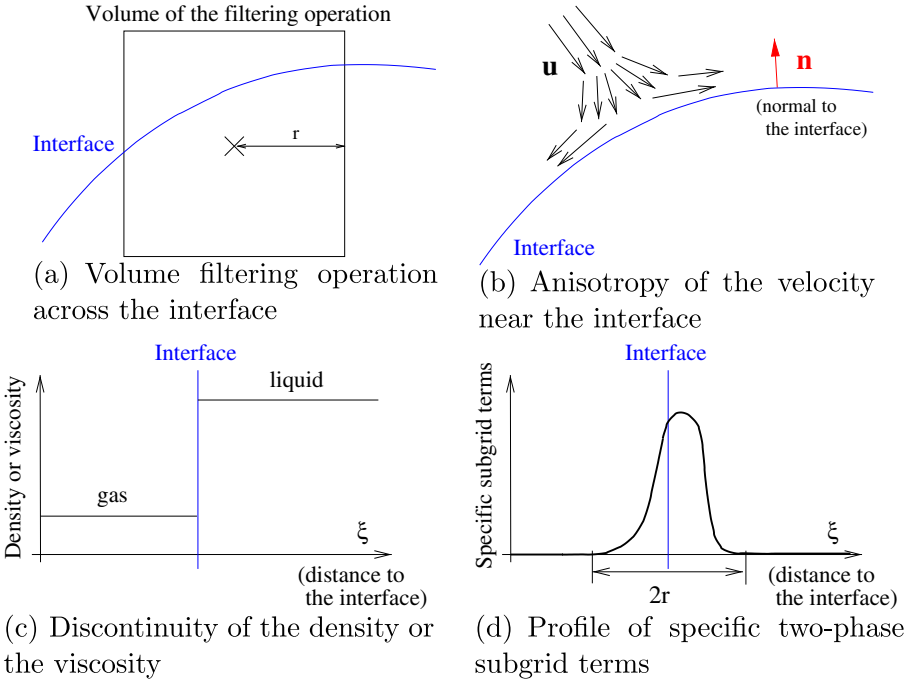

(a) Volume filtering operation across the interface

(b) Anisotropy of the velocity near the interface

(c) Discontinuity of the density or the viscosity

(d) Profile of specific two-phase subgrid terms

Fig. 3. Origin of specific subgrid terms.

where G is the convolution kernel of the filtering operation[1] (Fig. 3). When G depends only on $(x^0 - x)$ and is independent of the time t, the volume filtering operation commutes with the spatial and the time derivatives. We also define a surface filtering operation $\bar{\cdot}^s$:

$$\bar{\phi}^s(x^0) = \begin{cases} \frac{\int_{\mathbb{R}^3} G(x^0-x)\,\phi(x)\,\delta_\sigma(x)dx}{\int_{\mathbb{R}^3} G(x^0-x)\,\delta_\sigma(x)dx} & \text{if} \quad \int_{\mathbb{R}^3} G(x^0-x)\delta_\sigma(x)dx \neq 0, \\ 0 & \text{otherwise.} \end{cases} \tag{4b}$$

This surface filtering operation is such that:

$$\overline{\phi\delta_\sigma}(x^0) = \bar{\phi}^s(x^0)\overline{\delta_\sigma}(x^0) \tag{5}$$

Applying the filtering operation (4a) to the one-fluid Eqs. (2), we obtain:

$$\nabla \cdot \bar{\mathbf{u}} = 0 \tag{6a}$$

$$\frac{\partial \overline{\chi_k}}{\partial t} + \bar{\mathbf{u}} \cdot \nabla \overline{\chi_k} + \tau_{interf} = 0 \tag{6b}$$

$$\begin{aligned} &\frac{\partial(\bar{\rho}\bar{\mathbf{u}} + \boldsymbol{\tau}_{temp})}{\partial t} + \nabla \cdot (\bar{\rho}\bar{\mathbf{u}} \otimes \bar{\mathbf{u}} + \boldsymbol{\tau}_{conv}) = -\nabla \bar{p} \\ &\quad + \nabla \cdot (\bar{\mu}(\nabla\bar{\mathbf{u}} + \nabla^T\bar{\mathbf{u}}) + \boldsymbol{\tau}_{diff}) + \bar{\rho}\mathbf{g} + \sigma\bar{\kappa}^s\bar{\mathbf{n}}^s\overline{\delta_\sigma} + \boldsymbol{\tau}_{superf} \end{aligned} \tag{6c}$$

where

$$\tau_{interf} = \overline{\mathbf{u} \cdot \nabla\chi_k} - \bar{\mathbf{u}} \cdot \nabla\overline{\chi_k} \tag{7a}$$

$$\boldsymbol{\tau}_{temp} = \overline{\rho\mathbf{u}} - \bar{\rho}\bar{\mathbf{u}} \tag{7b}$$

$$\boldsymbol{\tau}_{conv} = \overline{\rho\mathbf{u} \otimes \mathbf{u}} - \bar{\rho}\bar{\mathbf{u}} \otimes \bar{\mathbf{u}} \tag{7c}$$

$$\boldsymbol{\tau}_{diff} = \overline{\mu(\nabla\mathbf{u} + \nabla^T\mathbf{u})} - \bar{\mu}(\nabla\bar{\mathbf{u}} + \nabla^T\bar{\mathbf{u}}) \tag{7d}$$

$$\boldsymbol{\tau}_{superf} = \sigma\overline{\kappa\mathbf{n}\delta_\sigma} - \sigma\bar{\kappa}^s\bar{\mathbf{n}}^s\overline{\delta_\sigma} \tag{7e}$$

Using Eq. (5), one gets $\overline{\kappa\mathbf{n}\delta_\sigma} = \overline{\kappa\mathbf{n}}^s\overline{\delta_\sigma}$. Thus, the subgrid term related to the capillary force can be written:

$$\boldsymbol{\tau}_{superf} = \sigma(\overline{\kappa\mathbf{n}}^s - \bar{\kappa}^s\bar{\mathbf{n}}^s)\overline{\delta_\sigma} \tag{8}$$

τ_{interf} is the subgrid term related to the interface transport. This term is due to the correlations between the velocity and the normal to the interface. These correlations exist because the interface makes the velocity field anisotropic (Fig. 3). Obviously this term has a zero contribution far from the interface (Fig. 3). $\boldsymbol{\tau}_{temp}, \boldsymbol{\tau}_{conv}, \boldsymbol{\tau}_{diff}$ and $\boldsymbol{\tau}_{superf}$ are four specific tensors of the momentum balance equation associated respectively to acceleration, advection, viscous effects and capillary forces. Only the term related to advection $\boldsymbol{\tau}_{conv}$ exists for single-phase flows. Although in the single-phase case this term is due only to the velocity–velocity correlation, in the two-phase case it is due to the threefold density–velocity–velocity correlation. Consequently, a part of this term is specific to two-phase flows and is due to the density discontinuity. The three other terms are purely specific to two-phase flows. They are due to the discontinuity (Fig. 3) and have a zero contribution far from the interface (Fig. 3). All these subgrid terms involve non-filtered quantities and cannot be evaluated using only the filtered quantities. Thus, they have to be modeled. To minimize the modeling work, we sort out the subgrid terms of the momentum equation and exhibit the terms that can be neglected.

3.3. Ordering of the subgrid terms

If the flow is so that

- the interface curvature radius are much larger than the filter size and are not very distorted,
- the boundary layer at the interface is much larger than the filter size,

the *a priori* tests realized thanks to several DNS of different kind of flows give the following ordering for the magnitude of the different subgrid terms and their energetic contributions (Toutant et al., 2006; Toutant et al., 2008; Labourasse et al., 2007):

[1] This is a general writing of filtered quantities and the more classical expression $1/V \int_V \phi(y)dy$ enters into this general class, where V is the volume of the filtering operation, *e.g.*, (Toutant et al., 2008).

$$\|\nabla\cdot(\boldsymbol{\tau}_{conv})\| > \left\|\frac{\partial\boldsymbol{\tau}_{temp}}{\partial t}\right\| \gg \|\nabla\cdot(\boldsymbol{\tau}_{diff})\| \gg \|\boldsymbol{\tau}_{superf}\| \tag{9a}$$

$$|\boldsymbol{\tau}_{conv}:\nabla\mathbf{u}| > \left|\frac{\partial\boldsymbol{\tau}_{temp}}{\partial t}\cdot\mathbf{u}\right| \gg |\boldsymbol{\tau}_{diff}:\nabla\mathbf{u}| \gg |\boldsymbol{\tau}_{superf}\cdot\mathbf{u}| \tag{9b}$$

Consequently, we neglect the subgrid terms related to the viscous effect $\boldsymbol{\tau}_{diff}$ and to the capillary forces $\boldsymbol{\tau}_{superf}$. The three other terms, τ_{interf}, $\boldsymbol{\tau}_{temp}$ and $\boldsymbol{\tau}_{conv}$, have to be modeled.

3.4. Closures

The three subgrid terms, τ_{interf}, $\boldsymbol{\tau}_{temp}$ and $\boldsymbol{\tau}_{conv}$ need to be modeled. For this, we propose to use a scale similarity hypothesis of the same type as in single-phase LES modeling. The similarity hypothesis of the LES is based on the fact that the largest non-resolved scales of the flow act similarly to the smallest resolved scales. Mathematically, the scale similarity models could be assimilated to techniques of reconstruction (Sagaut, 2003). We thus propose the following models:

$$\tau^{meso}_{interf} = \overline{\bar{\mathbf{u}}\cdot\nabla\overline{\chi_k}} - \bar{\bar{\mathbf{u}}}\cdot\nabla\overline{\overline{\chi_k}} \tag{10a}$$

$$\boldsymbol{\tau}^{meso}_{temp} = \overline{\bar{\rho}\bar{\mathbf{u}}} - \bar{\bar{\rho}}\bar{\bar{\mathbf{u}}} \tag{10b}$$

$$\boldsymbol{\tau}^{meso}_{conv} = \overline{\bar{\rho}\bar{\mathbf{u}}\otimes\bar{\mathbf{u}}} - \bar{\bar{\rho}}\bar{\bar{\mathbf{u}}}\otimes\bar{\bar{\mathbf{u}}} \tag{10c}$$

However, if one aims at validating the scale similarity hypothesis point by point, the presence of discontinuities and the double-filtering operation of the scale similarity hypothesis raise the following issue. The terms that need to be modeled are non-zero only in a region of thickness δ surrounding the interface, where δ is the size of the filter (see Eq. (7e)). Now, because the scale similarity hypothesis is based on a double-filtering operation, the corresponding terms are non-zero on a region of thickness 2δ surrounding the interface (see Eq. (10c)). Therefore, to perform a point to point validation of the model, it is necessary to adapt the scale similarity hypothesis. This has been done and validated in our previous work (Toutant et al., 2006; Toutant et al., 2008), where we proposed the following model:

$$\tau^{ve}_{interf} = \overline{\bar{\mathbf{u}}\cdot\nabla\chi_k} - \bar{\bar{\mathbf{u}}}\cdot\nabla\overline{\chi_k} \tag{11a}$$

$$\boldsymbol{\tau}^{ve}_{temp} = \overline{\rho\bar{\mathbf{u}}} - \bar{\rho}\bar{\bar{\mathbf{u}}} \tag{11b}$$

$$\boldsymbol{\tau}^{ve}_{conv} = \overline{\rho\bar{\mathbf{u}}\otimes\bar{\mathbf{u}}} - \bar{\rho}\bar{\bar{\mathbf{u}}}\otimes\bar{\bar{\mathbf{u}}} \tag{11c}$$

The superscript ve means *validated expressions*. The main idea behind this new decomposition is the following (see Toutant et al., 2006; Toutant et al., 2008 for details). The scale similarity hypothesis consists in neglecting the Reynolds and cross terms compared to the Leonard term in the Leonard and Germano decomposition. Here, we make the same hypothesis with a new decomposition where, in the Leonard term, the discontinuous quantities (*i.e.* density and the phase indicator function) are filtered only one time. Thanks to this new decomposition, the *Leonard term is equal to zero when the subgrid term is equal to zero*. Furthermore, we have shown using several *a priori* tests that these expressions are valid and very well correlated point to point to the subgrid terms (Toutant et al., 2006; Toutant et al., 2008; Labourasse et al., 2007).

Thus, the expressions (11c) are valid in the transition region and are zero when the subgrid terms are zero. However, these expressions are not totally closed since they involve microscopic quantities (namely χ_k and ρ). Now, a closed model is needed at the mesoscopic scale, in particular, in this study, to perform the second up-scaling step. It turns out that, in the second up-scaling step, the physical quantities defined in the interfacial region will be integrated over the interfacial transition region to be assigned to the interface through corresponding surface-excess quantities. Thus, to obtain a validated closed model at the mesoscopic scale, we need expressions whose integral over the interfacial thickness is equal (at a given order) to the integral of the point to point validated model (11c) (that is not closed at the mesoscopic scale). We can show that the scale similarity model (10c) satisfies this condition, at least at the dominant order of the matched asymptotic expansion (see Appendix B for the proof of this property). At this stage, the scale similarity model is validated in the sense that its integral over the interface thickness is equal to the integral of the point to point validated model and thus to the integral of the original subgrid term (7e). This is why the scale similarity hypothesis (10c) is used to close the system at the mesoscopic scale.

For the capillary force term $\sigma\bar{\kappa}^s\bar{\mathbf{n}}^s\overline{\delta_\sigma}$, using Eqs. (3) and (5), and the fact that the filtering operation commutes with the spatial derivatives, one gets:

$$\bar{\mathbf{n}}^s\overline{\delta_\sigma} = \overline{\mathbf{n}\,\delta_\sigma} = -\nabla\overline{\chi_g} \tag{12}$$

Regarding the curvature, the quantity $\bar{\kappa}^s$ is not closed at the mesoscopic scale. It depends on the unknown microscopic quantity κ. Thus, we introduce another estimate of the curvature at the mesoscopic scale $\kappa_{\bar{\chi}}$, which is closed and defined in the transition region as:

$$\kappa_{\bar{\chi}} = -\nabla\cdot\mathbf{n}_{\bar{\chi}} \quad \text{where} \quad \mathbf{n}_{\bar{\chi}} = -\frac{\nabla\overline{\chi_g}}{|\nabla\overline{\chi_g}|} \tag{13}$$

We showed in the previous section that the subgrid term associated to the capillary force is negligible. Using this new estimation of the mesoscopic curvature in the subgrid term $\boldsymbol{\tau}_{superf} = \sigma(\bar{\kappa}\bar{\mathbf{n}}^s - \kappa_{\bar{\chi}}\bar{\mathbf{n}}^s)\overline{\delta_\sigma}$ should not change the order of magnitude of this term, which remains negligible.

Using the model (10c), Eq. (12) and the new estimation of the mesoscopic curvature, the system (6) becomes:

$$\nabla\cdot\bar{\mathbf{u}} = 0 \tag{14a}$$

$$\frac{\partial\overline{\chi_k}}{\partial t} + \bar{\mathbf{u}}\cdot\nabla\overline{\chi_k} + \overline{\bar{\mathbf{u}}\cdot\nabla\overline{\chi_k}} - \bar{\bar{\mathbf{u}}}\cdot\nabla\overline{\overline{\chi_k}} = 0 \tag{14b}$$

$$\begin{aligned}\frac{\partial\bar{\rho}\bar{\mathbf{u}}}{\partial t} + \nabla\cdot(\bar{\rho}\bar{\mathbf{u}}\otimes\bar{\mathbf{u}}) = {} & -\nabla\bar{p} + \frac{\partial\bar{\bar{\rho}}\bar{\bar{\mathbf{u}}} - \overline{\bar{\rho}\bar{\mathbf{u}}}}{\partial t} + \nabla\cdot(\bar{\bar{\rho}}\bar{\bar{\mathbf{u}}}\otimes\bar{\bar{\mathbf{u}}} \\ & - \overline{\bar{\rho}\mathbf{u}\otimes\bar{\mathbf{u}}}) + \nabla\cdot(\bar{\mu}(\nabla\bar{\mathbf{u}} + \nabla^T\bar{\mathbf{u}})) \\ & + \bar{\rho}\mathbf{g} - \sigma\kappa_{\bar{\chi}}\nabla\overline{\chi_g}\end{aligned} \tag{14c}$$

At this stage, the equations at the mesoscopic or continuous LES level are closed. They do not depend on any non-filtered quantity. We remind that the specific subgrid terms, τ^{meso}_{interf} and $\boldsymbol{\tau}^{meso}_{temp}$ (closed by Eqs. (10a) and (10b), respectively), have a zero contribution far from the interface and that they represent the coupling between turbulence and interfaces in the continuous transition zone. However, as underlined in the introduction, we do not aim at solving the problem at this level of description where the interface is a continuous transition zone. For numerical reasons, we aim at stiffening the interface. It is the purpose of the following section.

4. Interface and subgrid scales

This section deals with the up-scaling from the continuous LES to the macroscopic or ISS level. During this up-scaling, the transition zone becomes again a discontinuity surface. The challenge of the ISS concept is to determine

- the jump conditions at the under-resolved discontinuous interface that take into account the interaction between turbulence and interfaces,
- the transport equation of the under-resolved discontinuous interface.

As we will see, the jump conditions and the velocity of the equivalent interface depend on the model related to the acceleration subgrid term τ_{temp}^{meso} and the model related to the interface transport τ_{interf}^{meso} respectively.

4.1. Form of the sought jump conditions

Before closing the jump conditions of the ISS level, their form has to be determined first. The issue is the following: considering two domains with their own equations, what expressions must be modeled at their mutual boundary to close the problem?

In our case, the two domains are the domain of liquid and the domain of the gas. The equations in each phase correspond to the system (14) when we are far from the interface. In each phase far from the interface, the density, ρ, and the viscosity, μ, are constant and the term related to surface tension is equal to zero. The fact that the density is constant in each phase implies in particular that the subgrid term related to acceleration is zero far from the interface:

$$\frac{\partial \boldsymbol{\tau}_{temp}^{meso}}{\partial t} = \frac{\partial \overline{\overline{\rho}\,\overline{\mathbf{u}}} - \overline{\overline{\rho}}\,\overline{\overline{\mathbf{u}}}}{\partial t} = 0 \tag{15}$$

Noting respectively the velocity and the pressure of the filtered problem at the ISS level $\tilde{\mathbf{u}}_k$ and $\tilde{p}_k$, in each phase k far from the interface, the system (14) degenerates to:

$$\nabla \cdot \tilde{\mathbf{u}}_k = 0 \tag{16a}$$

$$\frac{\partial \rho_k \tilde{\mathbf{u}}_k}{\partial t} + \nabla \cdot (\rho_k \tilde{\mathbf{u}}_k \otimes \tilde{\mathbf{u}}_k) = -\nabla \tilde{p}_k + \nabla \cdot (\mu_k (\nabla \tilde{\mathbf{u}}_k + \nabla^T \tilde{\mathbf{u}}_k)) + \nabla \cdot (\rho_k (\widetilde{\overline{\mathbf{u}}_k} \otimes \widetilde{\overline{\mathbf{u}}_k} - \widetilde{\overline{\mathbf{u}}_k} \otimes \widetilde{\overline{\mathbf{u}}_k})) \tag{16b}$$

These equations are those of the single-phase LES when one uses the scale similarity hypothesis. However, these equations have to be solved up to the interface and not only far away from the discontinuity. Consequently, this single-phase system is extended until the interface to define the macroscopic governing equations in each phase. Doing this, errors in term of interfacial transfers are necessarily done in the interfacial region. However, these interfacial transfers not taken into account by the macroscopic model compared to the mesoscopic one will be assigned to the interface through the jump conditions.

The form of the sought jump conditions is determined using the one-fluid formalism. As we have seen, this formalism consists in using only one physical variable for the gas and the liquid thanks to a phase indicator function. At the ISS level, the phase indicator function is discontinuous but may be different from the one of the DNS level. The precise definition of this phase indicator function is related to the transport of the under-resolved discontinuous interface. It is an important modeling issue that we will consider later. At this step we just note the phase indicator function $\tilde{\chi}_k$ and define the one-fluid variable of the ISS level $\tilde{\phi}$ by $\tilde{\phi} \hat{=} \sum_k \widetilde{\chi_k}\widetilde{\phi_k}$. Let us also note:

$$\widetilde{\mathscr{L}}_k \hat{=} \widetilde{\overline{\mathbf{u}}_k} \otimes \widetilde{\overline{\mathbf{u}}_k} - \widetilde{\overline{\mathbf{u}}_k} \otimes \widetilde{\overline{\mathbf{u}}_k}$$

$$\widetilde{\mathbf{S}}_k \hat{=} \mu_k \left(\nabla \widetilde{\mathbf{u}_k} + \nabla^T \widetilde{\mathbf{u}_k} \right)$$

Multiplying Eqs. (16a) and (16b) by the discontinuous filtered phase indicator function, $\tilde{\chi}_k$, and summing each of them over k, we obtain the following equations:

$$\nabla \cdot \tilde{\mathbf{u}} - \sum_k \widetilde{\mathbf{u}_k} \cdot \nabla \widetilde{\chi_k} = 0 \tag{17a}$$

$$\frac{\partial \tilde{\rho}\tilde{\mathbf{u}}}{\partial t} + \nabla \cdot (\tilde{\rho}\tilde{\mathbf{u}} \otimes \tilde{\mathbf{u}}) = -\nabla \tilde{p} + \nabla \cdot (\widetilde{\mathbf{S}}) + \nabla \cdot (\tilde{\rho}\widetilde{\mathscr{L}}) + \sum_k \left(\rho_k \widetilde{\mathbf{u}_k} \frac{\partial \widetilde{\chi_k}}{\partial t} + (\widetilde{p_k}\mathbf{I} - \widetilde{\mathbf{S}}_k + \rho_k (\widetilde{\mathbf{u}_k} \otimes \widetilde{\mathbf{u}_k} - \widetilde{\mathscr{L}}_k)) \cdot \nabla \widetilde{\chi_k} \right) \tag{17b}$$

These equations allow to determine the form of the boundary conditions. Indeed, the boundary conditions are the jump of the normal velocity (boxed term of Eq. (17a)) and the jump of the momentum tensors (boxed term of Eq. (17b)). The previous system is not closed. Indeed, we exhibit the form of the boundary conditions (boxed terms) but they are not expressed as function of the one-fluid variables. The next step consists in using the continuous equations near the interface to determine the jump conditions as functions of the specific subgrid terms. We remind that in DNS case (*i.e.* at the microscopic level), we have:

- jump condition related to mass conservation

$$\sum_k \mathbf{u}_k \cdot \nabla \chi_k = 0 \tag{18a}$$

- jump condition related to momentum conservation

$$\sum_k (p_k \mathbf{I} - \mathbf{S}_k) \cdot \nabla \chi_k = -\sigma (\nabla_s \cdot \mathbf{n}) \mathbf{n} \delta_\sigma = \sigma \kappa \mathbf{n} \delta_\sigma \tag{18b}$$

These conditions must be satisfied at the interface that is implicitly defined by its transport equation:

$$\frac{\partial \chi_k}{\partial t} + \mathbf{u} \cdot \nabla \chi_k = 0 \tag{18c}$$

In diffuse interface models (Emmerich, 2003), the DNS jump conditions are recovered by looking for the sharp-interface limit when the thickness of the transition zone tends to zero. The major aim of the present contribution is to find the jump conditions that the LES equations with continuous interfaces exhibit when the interface thickness tends to zero: what is the equivalent of the jump conditions (18a) valid for the DNS scale for the filtered LES quantities? As shown in the system (17), one has to determine:

- the jump condition related to the filtered mass equation

$$\sum_k \widetilde{\mathbf{u}_k} \cdot \nabla \widetilde{\chi_k} \tag{19a}$$

- the jump condition related to the filtered momentum equation

$$\sum_k \left(\rho_k \widetilde{\mathbf{u}_k} \frac{\partial \widetilde{\chi_k}}{\partial t} + (\widetilde{p_k}\mathbf{I} - \widetilde{\mathbf{S}}_k + \rho_k (\widetilde{\mathbf{u}_k} \otimes \widetilde{\mathbf{u}_k} - \widetilde{\mathscr{L}}_k)) \cdot \nabla \widetilde{\chi_k} \right) \tag{19b}$$

These jump conditions will be imposed at the under-resolved discontinuous interface. The under-resolved discontinuous interface is formally defined by the following transport equation

$$\frac{\partial \widetilde{\chi_k}}{\partial t} + \mathbf{v}_{\tilde{\sigma}} \cdot \nabla \widetilde{\chi_k} = 0 \tag{19c}$$

where $\mathbf{v}_{\tilde{\sigma}}$ is the velocity of the under-resolved discontinuous interface, $\widetilde{\chi_k}$. Expressing the velocity, $\mathbf{v}_{\tilde{\sigma}}$, of the equivalent discontinuity, $\widetilde{\chi_k}$, (Eq. (19c)) allows to follow the location where the jump conditions have to be imposed. This step is as difficult as essential. It is essential because a major objective is obviously the precise prediction of the location of the interface. It is difficult because the interface location depends on the effect of the subgrid velocity fluctuations. Consequently, the velocity of the equivalent discontinuity is different from the filtered one-fluid velocity.

In the following, we show that applying the method of the matched asymptotic expansions to the equations of the continuous LES allows to close the equivalent discontinuous problem by providing closure relations for the system (19).

4.2. Matched asymptotic expansions

To perform the up-scaling from the continuous interface to the sharp-interface limit, we use the method of matched asymptotic expansions. This method is classical (Van Dyke, 1975; Zeytounian, 1986; Zwillinger, 1989) for the resolution of differential equations in which a small parameter ϵ is present. It is commonly used to study diffuse interface problems, *e.g.* (Emmerich, 2003). It is based on the following idea. An approximated problem of the continuous problem is derived using a matched asymptotic expansion as the interface thickness tends towards zero. This obtained approximated problem is discontinuous, is build such that it is a good approximation (at a given order) of the continuous problem, and its jump conditions at the interface are explicit. Thus, this method allows to find the sharp-interface limit of continuous diffuse interface problems.

More precisely, this method consists in dividing the resolution domain of the mesoscopic level in different subregions: an outer region, where the variables of the system are slowly varying and an inner region, where these variables are rapidly varying. In our study, the region where the filtering of the phase indicator function is different from one or zero corresponds to the inner region where the filtered density and viscosity are rapidly varying, while each single-phase region (liquid or gas) is an outer region where the density and the viscosity are constant. Then, a change of variable is made in the inner region, since variations of order one are expected to occur in this thin region. The solutions of the differential equations are studied separately in each region, using an asymptotic expansion and are then matched using matching principles.

This method is founded on Taylor expansions of partial derivative equations as a function of a small parameter: the non-dimensional interface thickness, ϵ. This small parameter is defined by the comparison of two different characteristic length scales. In our study, the large and small length scales correspond respectively to the local radius of the interface R_b and the thickness of the interfacial transition zone δ. Using these length scales, we have $\epsilon = \frac{\delta}{R_b}$. This length scale analysis requires non-dimensional equations.

4.2.1. Non-dimensional equations

The equations that are made non-dimensional govern the flow at the continuous LES level (system (14)). This step is very important because it determines the Taylor expansions and thus the results. We use the following notation:

- R_b, local radius of the osculatory sphere to the interface,
- V_T, bubble terminal velocity,
- δ, thickness of the transition zone, *i.e.* the filter size,
- g_n, norm of the vector gravity,
- ρ_l and μ_l density and dynamic viscosity of the liquid phase.[2]

We introduce the following non-dimensional quantities:

- $\nabla = \frac{1}{R_b}\nabla^+$,
- $\mathbf{u} = V_T\mathbf{u}^+$,
- $t = \frac{\delta}{V_T}t^+$,
- $p = \rho_l V_T^2 p^+$,
- $\rho = \rho_l\rho^+$ and $\mu = \mu_l\mu^+$.

[2] We choose the values of the liquid phase to make non-dimensional the equations because the non-dimensional numbers dedicated to study bubbly flows are based on the liquid phase characteristics.

The previous definition of the non-dimensional time t^+ is founded on the characteristic scale corresponding to the thickness of the transition zone δ. It is a choice because it is also possible to use the characteristic scale corresponding to the radius of the osculatory sphere R_b. This choice is motivated by the fact that the non-dimensional time, t^+, appears only when the thickness of the transition zone δ is concerned. Typically, it is the case of the subgrid term related to the acceleration τ_{temp} (Eq. (6c)) and of the term related to the time evolution of the phase indicator $\overline{\chi}_k$ (Eq. (6b)). The non-dimensional numbers required to write the non-dimensional equations are:

- the small parameter $\epsilon = \frac{\delta}{R_b}$,
- the Reynolds number $Re = \frac{\rho_l V_T R_b}{\mu_l}$,
- the Froude number $Fr = \frac{V_T}{\sqrt{g_n R_b}}$,
- and the Weber number $We = \frac{\rho_l V_T^2 R_b}{\sigma}$.

In the following, we omit the superscript + to lighten the notation. Because gravity does not introduce any closure issue, we consider (without loss of generality) non-gravitational flows. The dimensionless form of the system (14) is given by:

$$\nabla\cdot\bar{\mathbf{u}} = 0 \tag{20a}$$

$$\frac{1}{\epsilon}\frac{\partial\overline{\chi}_k}{\partial t} + \bar{\mathbf{u}}\cdot\nabla\overline{\chi}_k + \overline{\bar{\mathbf{u}}\cdot\nabla\chi_k} - \bar{\bar{\mathbf{u}}}\cdot\nabla\overline{\overline{\chi}_k} = 0 \tag{20b}$$

$$\begin{aligned}\frac{1}{\epsilon}\frac{\partial\bar{\rho}\bar{\mathbf{u}}}{\partial t} + \nabla\cdot(\bar{\rho}\bar{\mathbf{u}}\otimes\bar{\mathbf{u}}) = &-\nabla\bar{p} + \frac{1}{\epsilon}\frac{\partial(\bar{\bar{\rho}}\bar{\bar{\mathbf{u}}} - \overline{\bar{\rho}\bar{\mathbf{u}}})}{\partial t}\\ &+\nabla\cdot(\bar{\bar{\rho}}\bar{\bar{\mathbf{u}}}\otimes\bar{\bar{\mathbf{u}}} - \overline{\bar{\rho}\bar{\mathbf{u}}\otimes\bar{\mathbf{u}}})\\ &+\frac{1}{Re}\nabla\cdot(\bar{\mu}(\nabla\bar{\mathbf{u}} + \nabla^T\bar{\mathbf{u}})) - \frac{\kappa_{\bar{\chi}}}{We}\nabla\overline{\chi}_g\end{aligned} \tag{20c}$$

The multiplication factor $1/\epsilon$ of the time derivative terms (the first term of the left hand side of the transport of the filtered phase indicator (20a), the first term of the left side and the second term of the right hand side of the momentum Eq. (20b)) is due to the characteristic length scale of these terms. Indeed, because these three terms involve the filtered phase indicator function, we can consider that their characteristic length scale is the thickness of the transition zone. The first term of the left hand side of the transport of the filtered phase indicator (20a) and the second term of the right hand side of the momentum Eq. (20b) only exist into the inner region (they are equal to zero in the outer region because $\bar{\chi} = cte$ and $\rho = \bar{\rho}$). Thus, their characteristic length scale must be the thickness of the transition zone. However, the first term of the left hand side of the momentum Eq. (20b) exists both in the inner and outer regions. Consequently, its characteristic length could be the macroscopic length scale R_b or the microscopic one δ. Because we focus our study on the interface, we choose to make this term non-dimensional using the microscopic length scale (the same length scale as for the other terms). We will show that this choice implies that at order zero in ϵ the **macroscopic** velocity is stationary. This means that interfacial phenomena and especially the time evolution of the phase indicator function (*i.e.* the transport of the interface) are very fast compared to the phenomena of the outer regions and especially the time evolution of the macroscopic velocity. Consequently, in first approximation, the interface is moved by a stationary velocity.

To study the system (20c), we need to work with orthogonal curvilinear coordinates to dissociate the tangential and normal directions. We choose the orthogonal curvilinear coordinates (ξ_1, ξ_2, ξ_3) associated to the ISS filtered discontinuous interface $\widetilde{\chi}_g$ (see Appendix A for the definitions and properties of the local orthogonal curvilinear coordinates). The ISS filtered discontinuous

surface cannot be explicitly defined at this stage. It will be defined later in Section 4.3.1. However we know that it is located within the transition region, close to the surface $\overline{\chi}_g = 1/2$.(ξ_1, ξ_2) are the surface coordinates related to the directions of the principal curvatures and ξ_3 is the signed distance to the interface (Fig. 4). In the following sections, we also use the scale factors or Lamé coefficient of each principal directions h_1 and h_2 and the principal curvatures κ_1 and κ_2 (Appendix A).

4.2.2. Inner region

To study the inner region, a new space variable that widens the coordinate normal to the interface is introduced. This new space variable allows to make interfacial phenomena preponderant. It is defined by:

$$\xi \hat{=} \frac{\xi_3}{\epsilon}, \quad \text{with} \quad \epsilon \hat{=} \frac{\delta}{R_b} \tag{21}$$

Let ϕ be any physical variables. In the inner region, we introduce $\breve{\phi}$

$$\breve{\phi}(\xi_1, \xi_2, \xi) = \phi\left(\xi_1, \xi_2, \frac{\xi_3}{\epsilon}\right) \tag{22}$$

and the solution of the system (20) is sought for in the form:

$$\breve{\phi}(\xi_1, \xi_2, \xi, \epsilon) = \breve{\phi}^0(\xi_1, \xi_2, \xi) + \epsilon\,\breve{\phi}^1(\xi_1, \xi_2, \xi) + \epsilon^2\,\breve{\phi}^2(\xi_1, \xi_2, \xi) + \mathcal{O}(\epsilon^3) \tag{23}$$

To expand the system (20) in the inner region, we need to specify the density and viscosity variation in the inner region. The filtered phase indicator function $\bar{\chi}$ on which the density and the viscosity depend, is rapidly varying in the direction normal to the interface in the inner region. At this point, we only assume that this function varies as $\xi = \xi_3/\epsilon$. It only implies that the filtered phase indicator function $\breve{\bar{\chi}}$ (and thus $\breve{\rho}$ and $\breve{\mu}$) does not depend on ϵ and thus that series of $\breve{\bar{\chi}}_k$ on ϵ is reduced to the order zero: $\breve{\bar{\chi}}_k = \breve{\bar{\chi}}^0_k$.

In the following, the system (20c) is written using the new variable ξ defined above. A multiplication factor $1/\epsilon$ thus appears in front of spatial derivatives along the normal direction. These terms are preponderant and allow to define a simplified system.

4.2.2.1. Incompressibility constraint. Let us note $\breve{u}(i)$ the ith component of the vector $\breve{\mathbf{u}}$ in the orthogonal curvilinear coordinates associated to the interface $\{\mathbf{g}_i\}$ (Appendix A). In this basis, we have:

$$\nabla\cdot\breve{\mathbf{u}} = \frac{1}{h_1h_2}\left[h_2\frac{\partial\breve{u}(1)}{\partial\xi_1} + h_1\frac{\partial\breve{u}(2)}{\partial\xi_2} + h_1h_2\frac{1}{\epsilon}\frac{\partial\breve{u}(3)}{\partial\xi} - \breve{u}(3)(\kappa_1h_2 + \kappa_2h_1) - \epsilon\,\xi\left(\breve{u}(1)\frac{\partial\kappa_2}{\xi_1} + \breve{u}(2)\frac{\partial\kappa_1}{\xi_2}\right)\right] = 0 \tag{24}$$

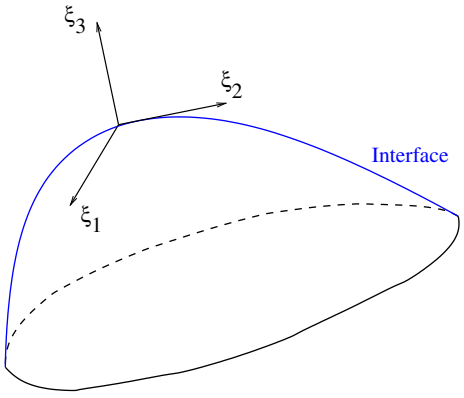

Fig. 4. Orthogonal curvilinear coordinates.

Applying the relation (23) to $\phi = \bar{u}(i)$ in the Eq. (24) multiplied by h_1h_2 and using the Taylor expansion of h_i in $\epsilon(h_i = 1 - \epsilon\xi\kappa_i + \mathcal{O}(\epsilon^2), i = 1, 2)$, one finds:

- **order 0**

$$\frac{\partial\breve{u}^0(3)}{\partial\xi} = 0 \tag{25a}$$

- **order 1** (using (25a))

$$\frac{\partial\breve{u}^0(1)}{\partial\xi_1} + \frac{\partial\breve{u}^0(2)}{\partial\xi_2} + \frac{\partial\breve{u}^1(3)}{\partial\xi} - \breve{u}^0(3)(\kappa_1 + \kappa_2) = 0 \tag{25b}$$

Eq. (25a) shows that at order zero the normal velocity is constant in the direction normal to the interface.

4.2.2.2. Conservation of momentum. Let us note

$$\mathbf{T} \hat{=} \boldsymbol{\tau}^{meso}_{temp} = \overline{\bar{\rho}\bar{\mathbf{u}}} - \bar{\rho}\bar{\mathbf{u}} \tag{26a}$$

$$\mathbf{C} \hat{=} \boldsymbol{\tau}^{meso}_{conv} = \overline{\bar{\rho}\bar{\mathbf{u}}\otimes\bar{\mathbf{u}}} - \bar{\rho}\bar{\mathbf{u}}\otimes\bar{\mathbf{u}} \tag{26b}$$

$$\breve{\mathbf{T}} \hat{=} \overline{\breve{\bar{\rho}}\breve{\bar{\mathbf{u}}}} - \breve{\bar{\rho}}\breve{\bar{\mathbf{u}}} \tag{26c}$$

$$\breve{\mathbf{C}} \hat{=} \overline{\breve{\bar{\rho}}\breve{\bar{\mathbf{u}}}\otimes\breve{\bar{\mathbf{u}}}} - \breve{\bar{\rho}}\breve{\bar{\mathbf{u}}}\otimes\breve{\bar{\mathbf{u}}} \tag{26d}$$

and for example $\mathbf{C}^0$ the order zero of the tensor $\mathbf{C}$. Furthermore to lighten the notation, let us write spatial derivatives along the direction i as follows:

$$\phi_{,i} \hat{=} \frac{\partial\phi}{\partial\xi_i} \tag{27}$$

Similarly to the incompressibility constraint and using Eq. (A.18a) the relation (20b) along $\mathbf{g}_1$ yields:

- **order 0**

$$\left(\breve{\mu}\breve{u}^0(1)_{,3}\right)_{,3} = 0 \tag{28a}$$

- **order 1**

$$\begin{aligned}\frac{\partial\breve{\rho}\breve{u}^0}{\partial t}(1) + (\breve{\rho}\breve{u}^0(1)\breve{u}^0(3))_{,3} = &-\frac{\partial\breve{T}^0}{\partial t}(1) - \left(\breve{C}^0_{13}\right)_{,3} \\ &+\frac{1}{Re}\left(\breve{\mu}\breve{u}^1(1)_{,3} + \breve{\mu}\breve{u}^0(3)_{,1} + \kappa_1\breve{\mu}\breve{u}^0(1)\right)_{,3} \\ &-\frac{\kappa_1}{Re}\left(\breve{\mu}\breve{u}^0(1)_{,3} + \xi\left(\breve{\mu}\breve{u}^0(1)_{,3}\right)_{,3}\right) \\ &-\frac{\kappa_1+\kappa_2}{Re}\left(\breve{\mu}\breve{u}^0(1)_{,3}\right)\end{aligned} \tag{28b}$$

Using (A.18b), the relation (20b) along $\mathbf{g}_2$ yields:

- **order 0**

$$\left(\breve{\mu}\breve{u}^0(2)_{,3}\right)_{,3} = 0 \tag{29a}$$

- **order 1**

$$\begin{aligned}\frac{\partial\breve{\rho}\breve{u}^0}{\partial t}(2) + \left(\breve{\rho}\breve{u}^0(2)\breve{u}^0(3)\right)_{,3} = &-\frac{\partial\breve{T}^0}{\partial t}(2) - \left(\breve{C}^0_{23}\right)_{,3} \\ &+\frac{1}{Re}\left(\breve{\mu}\breve{u}^1(2)_{,3} + \breve{\mu}\breve{u}^0(3)_{,2} + \kappa_2\breve{\mu}\breve{u}^0(2)\right)_{,3} \\ &-\frac{\kappa_2}{Re}\left(\breve{\mu}\breve{u}^0(2)_{,3} + \xi\left(\breve{\mu}\breve{u}^0(2)_{,3}\right)_{,3}\right) \\ &-\frac{\kappa_1+\kappa_2}{Re}\left(\breve{\mu}\breve{u}^0(2)_{,3}\right)\end{aligned} \tag{29b}$$

Using (A.18c), the relation (20b) along $\mathbf{g}_3$ yields:

- **order 0**

$$\left(\breve{\bar{\mu}}\breve{\bar{u}}^0(3)_{,3}\right)_{,3}=0 \tag{30a}$$

- **order 1**

$$\begin{aligned}\frac{\partial\breve{\bar{\rho}}\breve{\bar{u}}^0}{\partial t}(3)+\left(\breve{\bar{\rho}}\breve{\bar{u}}^0(3)\breve{\bar{u}}^0(3)\right)_{,3}=&-\frac{\partial\breve{T}^0}{\partial t}(3)-\left(\breve{C}^0_{33}\right)_{,3}-\breve{\bar{p}}^0_{,3}-\frac{1}{We}\breve{\kappa}^0_{\breve{\chi}}\breve{\chi}_{g,3}\\&+\frac{2}{Re}\left(\breve{\bar{\mu}}\breve{\bar{u}}^1(3)_{,3}\right)_{,3}+\frac{1}{Re}\left(\breve{\bar{\mu}}\breve{\bar{u}}^0(1)_{,3}\right)_{,1}\\&+\frac{1}{Re}\left(\breve{\bar{\mu}}\breve{\bar{u}}^0(2)_{,3}\right)_{,2}-\frac{\kappa_1+\kappa_2}{Re}\left(\breve{\bar{\mu}}\breve{\bar{u}}^0(3)_{,3}\right)\end{aligned} \tag{30b}$$

Eqs. (28a), (29a) and (30a) at order zero show that the viscous effect are preponderant in the interfacial region. We will see in Section 4.2.4.1 that it implies that, at order zero, the velocity does not depend on the normal coordinate ξ.

4.2.3. Outer region

In this region, we are far from the interfacial zone. The filtered phase indicator function and consequently the density and the viscosity are assumed to be constant in each phase. In this condition, the interfacial terms tend to zero and the system (20c) becomes:

$$\nabla\cdot\bar{\mathbf{u}}_k=0 \tag{31a}$$

$$\begin{aligned}\frac{1}{\epsilon}\frac{\partial\bar{\rho}_k\bar{\mathbf{u}}_k}{\partial t}+\nabla\cdot(\bar{\rho}_k\bar{\mathbf{u}}_k\otimes\bar{\mathbf{u}}_k)=&-\nabla\bar{p}_k+\nabla\cdot\left(\bar{\rho}_k\left(\overline{\bar{\mathbf{u}}_k\otimes\bar{\mathbf{u}}_k}-\overline{\bar{\mathbf{u}}_k}\otimes\overline{\bar{\mathbf{u}}_k}\right)\right)\\&+\frac{1}{Re}\nabla\cdot\left(\bar{\mu}_k\left(\nabla\bar{\mathbf{u}}_k+\nabla^T\bar{\mathbf{u}}_k\right)\right)\end{aligned} \tag{31b}$$

In particular, in the momentum equation, it is the subgrid term with the multiplication factor $1/\epsilon$ and the term related to the capillary forces that degenerates to zero. As expected given the construction of the macroscopic model, this system corresponds to the classical equations of LES single-phase flows when the scale similarity hypothesis is used. The solutions of the outer region are sought for in the form:

$$\phi_k(\xi_1,\xi_2,\xi_3,\epsilon)=\phi^0_k(\xi_1,\xi_2,\xi_3)+\epsilon\,\phi^1_k(\xi_1,\xi_2,\xi_3)+\mathcal{O}(\epsilon^2) \tag{32}$$

Using this relation does not modify the compressibility constraint. Whatever the order i in ϵ, one has:

$$\nabla\cdot\bar{\mathbf{u}}^i_k=0 \tag{33a}$$

It can be shown that the momentum equation yields the following equations:

- **order 0**

$$\frac{\partial\bar{\rho}_k\bar{\mathbf{u}}^0_k}{\partial t}=0 \tag{33b}$$

- **order** $i\geqslant 1$

$$\begin{aligned}\frac{\partial\bar{\rho}_k\bar{\mathbf{u}}^i_k}{\partial t}+\nabla\cdot(\bar{\rho}_k\bar{\mathbf{u}}^{i-1}_k\otimes\bar{\mathbf{u}}^{i-1}_k)=&-\nabla\bar{p}^{i-1}_k\\&+\nabla\cdot\left(\bar{\rho}_k\left(\bar{\bar{\mathbf{u}}}^{i-1}_k\otimes\bar{\bar{\mathbf{u}}}^{i-1}_k-\overline{\bar{\mathbf{u}}^{i-1}_k\otimes\bar{\mathbf{u}}^{i-1}_k}\right)\right)\\&+\frac{1}{Re}\nabla\cdot\left(\bar{\mu}_k\left(\nabla\bar{\mathbf{u}}^{i-1}_k+\nabla^T\bar{\mathbf{u}}^{i-1}_k\right)\right)\end{aligned} \tag{33c}$$

In each outer region, the flow is stationary at order zero in ϵ. It means that in first approximation -order zero- the time evolution of the interfacial phenomena is faster than the time evolution of the macroscopic quantities (*i.e.* quantities of the outer regions). Thus, at order zero, the interface is moved by a stationary velocity field.

4.2.4. Jump conditions

In order to solve completely the momentum equation and the incompressibility constraint in each region, boundary conditions are required. The missing boundary conditions are obtained by matching the solutions of the different regions. These matching conditions of any physical variable $\phi-\breve{\phi}$ in the inner region- are determined assuming that for the outer regions, the inner region is viewed as a surface located at $\xi_3=0$ and that in the inner region, the outer value is asymptotically reached:

$$\lim_{\xi\to\pm\infty}\breve{\phi}=\lim_{\xi_3\to 0^{\pm}}\phi \tag{34}$$

The above relation means that the parameter ϵ is small enough to allow $\xi_3\to 0$, although $\xi=\xi_3/\epsilon\to+\infty$. Identifying the coefficients of epsilon polynomial of $\breve{\phi}$ with the Taylor expansion of ϕ in zero (Fouillet, 2003; Zwillinger, 1989), one finds the following relations at order zero:

$$\lim_{\xi\to\pm\infty}\breve{\phi}^0=\lim_{\xi_3\to\ 0^{\pm}}\phi^0 \tag{35a}$$

$$\lim_{\xi\to\pm\infty}\frac{d\breve{\phi}^0}{d\xi}=0 \tag{35b}$$

$$\lim_{\xi\to\pm\infty}\frac{d\breve{\phi}^1}{d\xi}=\lim_{\xi_3\to 0^{\pm}}\frac{d\phi^0}{d\xi_3} \tag{35c}$$

4.2.4.1. Velocity jump conditions. In the inner region, the order zero of the momentum equation along the directions tangential to the interface (Eqs. (28a) and (29a)) yields

$$\breve{\bar{u}}^0(i)_{,3}=\frac{Ct_i}{\breve{\bar{\mu}}}\quad i=1,2 \tag{36}$$

where Ct_1 and Ct_2 are two functions independent of ξ. Because $\breve{\bar{\mu}}$ is bounded by μ_g and μ_l, the matching condition (35b) implies that $Ct_1=Ct_2=0$ and that:

$$\breve{\bar{u}}^0(i)_{,3}=0\quad i=1,2 \tag{37}$$

Consequently, $\breve{\bar{u}}^0(1)$ and $\breve{\bar{u}}^0(2)$ are independent of ξ.

The matching condition (35a) implies that the velocity components tangential to the interface are continuous at order zero:

$$\breve{\bar{u}}^0(1)=\bar{u}^0(1)|_+=\bar{u}^0(1)|_- \tag{38a}$$

$$\breve{\bar{u}}^0(2)=\bar{u}^0(2)|_+=\bar{u}^0(2)|_- \tag{38b}$$

Physically, we recover the classical jump conditions of the DNS level. In the tangential directions, the length scale δ, where the shear intervenes, is so small compared to the other characteristic length scales that any velocity gradients cannot develop. Consequently, there is no-slip between the two phases.

The order zero of the incompressibility constraint in the inner region (Eq. (25a)) implies that $\breve{\bar{u}}^0(3)$ is independent of ξ. According to the matching condition (35a), the normal component of the velocity is continuous at order zero:

$$\breve{\bar{u}}^0(3)=\bar{u}^0(3)|_+=\bar{u}^0(3)|_- \tag{38c}$$

The jump condition for the normal velocity corresponds also to the classical condition of the DNS level: the filtering operation does not introduce any subgrid mass or volume transfer.

Finally, at order zero, the jump condition for the filtered velocity is the same as for DNS:

$$\bar{\mathbf{u}}^0|_+-\bar{\mathbf{u}}^0|_-=0 \tag{39}$$

4.2.4.2. Tensor jump conditions. Using the fact that $\breve{\bar{\mathbf{u}}}^0$ is independent of ξ(Eq. (38)), Equations (28b), (29b) and (30b) become in a dimensional form:

$$\left(\breve{\bar{\mu}}\breve{\tilde{u}}^1(1)_{,3}\right)_{,3}+\left(\breve{\bar{\mu}}\breve{\tilde{u}}^0(3)_{,1}\right)_{,3}+\kappa_1\left(\breve{\bar{\mu}}\breve{\tilde{u}}^0(1)\right)_{,3}=\frac{\partial\breve{\bar{\rho}}\breve{\tilde{u}}^0}{\partial t}(1)+\frac{\partial\breve{\bar{T}}^0}{\partial t}(1)+\left(\breve{\bar{\rho}}\breve{\tilde{u}}^0(1)\breve{\tilde{u}}^0(3)+\breve{C}^0_{13}\right)_{,3} \tag{40a}$$

$$\left(\breve{\bar{\mu}}\breve{\tilde{u}}^1(2)_{,3}\right)_{,3}+\left(\breve{\bar{\mu}}\breve{\tilde{u}}^0(3)_{,2}\right)_{,3}+\kappa_2\left(\breve{\bar{\mu}}\breve{\tilde{u}}^0(2)\right)_{,3}=\frac{\partial\breve{\bar{\rho}}\breve{\tilde{u}}^0}{\partial t}(2)+\frac{\partial\breve{\bar{T}}^0}{\partial t}(2)+\left(\breve{\bar{\rho}}\breve{\tilde{u}}^0(2)\breve{\tilde{u}}^0(3)+\breve{C}^0_{23}\right)_{,3} \tag{40b}$$

$$-\breve{\bar{p}}^0_{,3}-\sigma\breve{\kappa}^0_{\breve{\chi}}\breve{\overline{\chi}}_{g,3}+2\left(\breve{\bar{\mu}}\breve{\tilde{u}}^1(3)_{,3}\right)_{,3}=\frac{\partial\breve{\bar{\rho}}\breve{\tilde{u}}^0}{\partial t}(3)+\frac{\partial\breve{\bar{T}}^0}{\partial t}(3)+\left(\breve{\bar{\rho}}\breve{\tilde{u}}^0(3)\breve{\tilde{u}}^0(3)+\breve{C}^0_{33}\right)_{,3} \tag{40c}$$

The matching conditions (35) make appear the order zero of the outer regions and the order 1 of the inner region. In order to use these relations, we combine these orders of the outer and inner regions. Integrating the subtraction between the Eqs. (40) related to the order 1 of the momentum balance equation in the inner region and Eq. (33b) related to the order zero in the outer region, the technical calculus presented in Appendix C finally give, using the original notations:

$$\left((\overline{\mathbf{S}}^0-\bar{p}^0\mathbf{I})|_+-(\overline{\mathbf{S}}^0-\bar{p}^0\mathbf{I})|_-\right)\cdot\tilde{\mathbf{n}}+\sigma\tilde{\kappa}\tilde{\mathbf{n}}-\left((\bar{\rho}\,\bar{\mathbf{u}}^0\otimes\bar{\mathbf{u}}^0+\boldsymbol{\tau}^{meso0}_{conv})|_+-(\bar{\rho}\,\bar{\mathbf{u}}^0\otimes\bar{\mathbf{u}}^0+\boldsymbol{\tau}^{meso0}_{conv})|_-\right)\cdot\tilde{\mathbf{n}}=\mathbf{I}_l+\mathbf{I}_g+\int_{-\infty}^{+\infty}\frac{\partial\boldsymbol{\tau}^{meso0}_{temp}}{\partial t}d\xi_3 \tag{41}$$

where $\mathbf{I}_l$ and $\mathbf{I}_g$ are defined by

$$\mathbf{I}_l=\int_0^{+\infty}\frac{\partial}{\partial t}\left(\breve{\bar{\rho}}\breve{\bar{\mathbf{u}}}^0-\rho_l\bar{\mathbf{u}}^0_l\right)d\xi \tag{42a}$$

$$\mathbf{I}_g=\int_{-\infty}^{0}\frac{\partial}{\partial t}\left(\breve{\bar{\rho}}\breve{\bar{\mathbf{u}}}^0-\rho_g\bar{\mathbf{u}}^0_g\right)d\xi \tag{42b}$$

The integrals appearing in the right hand side of Eq. (41) are the surface-excess quantities associated to the time evolution of $\rho\mathbf{u}$ and its associated subgrid term τ^{meso}_{temp}. As explained in Section 2.2, they take into account the coupling between turbulence and interface that is not seen by the macroscopic model in the transition zone and concentrate its effect at the discontinuity.

The ISS jump condition of the momentum (41) is similar to the DNS situation. However, the force at the interface is different. The three terms $\mathbf{I}_l+\mathbf{I}_g+\int_{-\infty}^{+\infty}\partial(\boldsymbol{\tau}^{meso0}_{conv})/\partial t\,d\xi_3$ added to the capillary forces take into account the defect of kinetic energy transfer at the interface. Contrary to the capillary forces these three terms have non-zero contribution in the tangential directions.

At this stage, the jump conditions of the velocity (39) and of the momentum (41) have been determined. These jump conditions allow to take into account the interfacial transfers not described by the macroscopic level compared to the mesoscopic one. Thus, the macroscopic problem is equivalent to the mesoscopic one. The discontinuity of the macroscopic level is a reconstruction of the interface inside the transition zone of the mesoscopic level. The jump conditions must be imposed at this equivalent interface. In the next section, we study the problem of the equivalent interface location (*i.e.* its transport equation).

4.2.5. Velocity of the filtered discontinuous interface

Because the interface allows to define the local orthogonal curvilinear coordinates, the transport equation of the interface is linked to the velocity of the local coordinates. To determine its velocity, we use the transport equation and the Lagrangian derivative (related to the local coordinates) of the filtered phase indicator function. Seeing that the interface is non-material, only the definition of the normal velocity is required. Using the transport equation of the interface at the mesoscopic level (20a), one gets at **order zero** (we recall that $\breve{\chi}_k=\breve{\chi}^0_k$):

$$\frac{\partial\breve{\overline{\chi}}_g}{\partial t}+\breve{\bar{\mathbf{u}}}^0\cdot\mathbf{g}_3\breve{\overline{\chi}}_{g,3}+\overline{\breve{\bar{\mathbf{u}}}^0\cdot\mathbf{g}_3\breve{\overline{\chi}}_{g,3}}-\overline{\breve{\bar{\mathbf{u}}}^0}\cdot\overline{\mathbf{g}_3\breve{\overline{\chi}}_{g,3}}=0 \tag{43}$$

To obtain the velocity of the filtered discontinuous interface, this equation is integrated along the normal direction. To perform this integration we have to permute time derivation and spatial integration, thus we first need to introduce the Lagrangian derivative D/Dt. Using the non-dimensional variable introduced in this paper, the link between the Eulerian derivative $\partial/\partial t$ and the Lagrangian derivative D/Dt is

$$\frac{1}{\epsilon}\frac{D\overline{\chi}_g}{Dt}=\frac{1}{\epsilon}\frac{\partial\bar{\chi}_g}{\partial t}\bigg|_{\mathbf{x}}+\mathbf{v}\cdot\nabla\bar{\chi}_g \tag{44}$$

where $\mathbf{v}$ is the velocity of the local coordinates $(\mathbf{g}_1,\mathbf{g}_2,\mathbf{g}_3)$. Let **OM** be the position vector, this velocity is:

$$\mathbf{v}=\frac{D\mathbf{OM}}{Dt} \tag{45}$$

Using the inner space variable $\xi\doteq\xi_3/\epsilon$ (Eq. (21)), Eq. (44) becomes at **order zero**:

$$\frac{D\breve{\overline{\chi}}_g}{Dt}=\frac{\partial\breve{\bar{\chi}}_g}{\partial t}\bigg|_{\mathbf{x}}+v^0_3\frac{\partial\breve{\bar{\chi}}_g}{\partial\xi} \tag{46}$$

Combining the Eqs. (43) and (46), one gets:

$$v^0_3\frac{\partial\breve{\bar{\chi}}_g}{\partial\xi}=\breve{\bar{\mathbf{u}}}^0\cdot\mathbf{g}_3\breve{\overline{\chi}}_{g,3}+\frac{D\breve{\overline{\chi}}_g}{Dt}+\overline{\breve{\bar{\mathbf{u}}}^0\cdot\mathbf{g}_3\breve{\overline{\chi}}_{g,3}}-\overline{\breve{\bar{\mathbf{u}}}^0}\cdot\overline{\mathbf{g}_3\breve{\overline{\chi}}_{g,3}} \tag{47}$$

In order to simplify the last two terms in the last equation, we introduce a filtering operation restricted to the surface (see Fig. 5). Let $\phi(\xi_1,\xi_2,\xi)$ be any physical variable continuous in particular across the interface. Using local orthogonal curvilinear coordinates, we define the filtering operation $\cdot^\sigma$ restricted to the surface in a non-dimensional form as

$$\bar{\phi}^\sigma(\xi^0_1,\xi^0_2)\doteq\int_{\mathbb{R}^2}G_\sigma(\xi^0_1-\xi_1,\xi^0_2-\xi_2)\phi(\xi_1,\xi_2,\xi=0)\,d\xi_1\,d\xi_2 \tag{48}$$

where G_σ is a two-dimensional convolution kernel. In this paper, we assume that the three-dimensional kernel $G(\xi_1,\xi_2,\xi)$ can be decomposed as $G(\xi_1,\xi_2,\xi)=G_{12}(\xi_1,\xi_2)\,G_3(\xi)$ where G_{12} and G_3 are two- and one-dimensional kernels, respectively. It means that the filtering operations in the tangential and in the normal directions are independent. This approximation is valid only if the principal curvatures of the interface are varying slowly in the direction normal to the interface over the filter size. Thus, we choose $G_\sigma=G_{12}$.

Using this filtering operation, the fact that the order zero of the velocity is constant in the inner region (38), the decomposition of the kernel G, the fact that $\breve{\overline{\chi}}_{g,3}$ does not depend on ξ_1 and ξ_2 over the filter size and the following equality

$$\int_{-\infty}^{+\infty}\frac{\partial\breve{\bar{\chi}}_g}{\partial\xi}d\xi=\chi_g|_+-\chi_g|_-=-1, \tag{49}$$

we deduce that:

$$\int_{-\infty}^{+\infty}\overline{\breve{\bar{\mathbf{u}}}^0\cdot\mathbf{g}_3\breve{\overline{\chi}}_{g,3}}d\xi=-\overline{\bar{\mathbf{u}}^0\cdot\mathbf{g}_3}^\sigma \tag{50}$$

and

$$\int_{-\infty}^{+\infty}\overline{\breve{\bar{\mathbf{u}}}^0}\cdot\overline{\mathbf{g}_3\breve{\overline{\chi}}_{g,3}}d\xi=-\overline{\bar{\mathbf{u}}^0}^\sigma\cdot\overline{\mathbf{g}_3}^\sigma \tag{51}$$

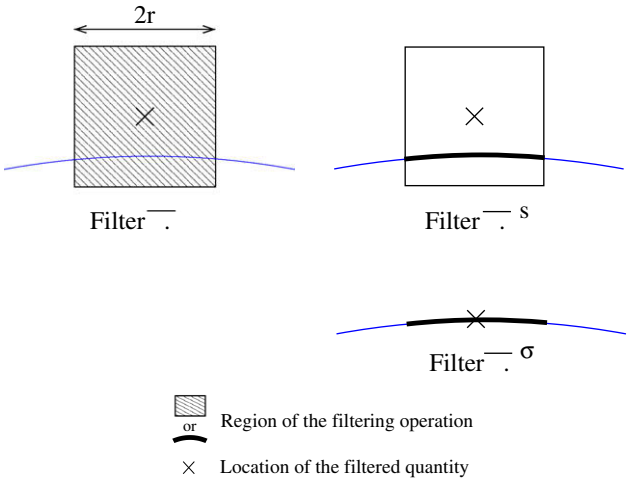

Fig. 5. Schematic representation of the different filtering operations.

Thus, the integral along the normal direction of Eq. (47) yields:

$$v_3^0(\xi_1,\xi_2) = \bar{\mathbf{u}}^0\cdot\mathbf{g}_3 - \int_{-\infty}^{+\infty}\frac{D\breve{\tilde{\chi}}_g}{Dt}d\xi + \overline{\bar{\mathbf{u}}^0\cdot\mathbf{g}_3}^{\sigma} - \overline{\bar{\mathbf{u}}^{0\sigma}}\cdot\overline{\mathbf{g}_3}^{\sigma} \tag{52}$$

To get the above equation, one uses the fact that the normal velocity v_3^0 does not depend on ξ_3. Indeed, using Eqs. (45) and (A.2), we have:

$$\begin{aligned}\frac{\partial v_3}{\partial\xi_3} &= \frac{\partial\mathbf{v}\cdot\mathbf{g}_3}{\partial\xi_3} = \frac{\partial\mathbf{v}}{\partial\xi_3}\cdot\mathbf{g}_3 + \mathbf{v}\cdot\frac{\partial\mathbf{g}_3}{\partial\xi_3} = \frac{\partial\mathbf{v}}{\partial\xi_3}\cdot\mathbf{g}_3\\ &= \frac{\partial}{\partial\xi_3}\left(\frac{D\mathbf{OM}}{Dt}\right)\cdot\frac{\partial\mathbf{OM}}{\partial\xi_3} = \frac{1}{2}\frac{D}{Dt}\left(\frac{\partial\mathbf{OM}}{\partial\xi_3}\cdot\frac{\partial\mathbf{OM}}{\partial\xi_3}\right)\\ &= \frac{1}{2}\frac{D(\mathbf{g}_3\cdot\mathbf{g}_3)}{Dt} = \frac{1}{2}\frac{D1}{Dt} = 0\end{aligned} \tag{53}$$

The relation (52) shows that in order to evaluate the velocity of the interface v_3^0 the normal fluid velocity must be corrected by taking into account the correlation between the velocity and the normal and the surface-excess quantity associated to the time evolution of the filtered phase indicator.

At this stage, the jump conditions at order zero have been determined. However, the surface-excess quantities $\mathbf{I}_l+\mathbf{I}_g$ in the momentum jump conditions (41) and $\int_{-\infty}^{+\infty}D\breve{\tilde{\chi}}_g/Dtd\xi$ in the transport Eq. (52) have to be closed. This is done in the following by defining the equivalent discontinuous problem at the macroscopic level.

4.3. Filtered discontinuous equations

4.3.1. Definition of the discontinuous problem

In Section 4.1, we introduced the notation $\sim$ to denote the physical quantities of the equivalent discontinuous problem that corresponds to the macroscopic level:

- the phase indicator function $\tilde{\chi}_g$,
- the pressure $\tilde{p}$ and
- the velocity $\tilde{\mathbf{u}}$.

Thanks to the matched asymptotic expansions, we determine the jump conditions of the outer region at order zero. We define the discontinuous problem as the order zero of the outer region.[3]

[3] It is a choice because the equivalent discontinuous problem could be defined at an arbitrary order of the outer region. To be more precise, it would be interesting to determine the jump conditions of the outer region at the order 1.

The velocity and the pressure are fully defined by the quantities of the outer region

$$\tilde{\mathbf{u}} \mathrel{\hat{=}} \bar{\mathbf{u}}^0 \tag{54a}$$

$$\tilde{p} \mathrel{\hat{=}} \bar{p}^0 \tag{54b}$$

but for $\tilde{\chi}_g$, we have a degree of freedom. Indeed, the boundary between the liquid and the gas phases at the macroscopic level could be everywhere inside the inner region of the mesoscopic level (Chandesris and Jamet, 2006; Chandesris and Jamet, 2007). In order to simplify the equations, we choose to impose local mass conservation

$$\int_V(\tilde{\chi}_g - \overline{\chi_g})dV = 0 \tag{55}$$

where V is the elementary control volume containing the inner region of the mesoscopic level. Because there is only one solution to conserve the local mass, this constraint defines $\tilde{\chi}_g$, *i.e.* the location of the equivalent discontinuous interface. The normal, $\tilde{\mathbf{n}}$, and the mean curvature, $\tilde{\kappa}$, of the filtered discontinuous interface are deduced from $\tilde{\chi}_g$ (and have already been used):

$$\tilde{\mathbf{n}}\delta_{\tilde{\sigma}} \mathrel{\hat{=}} -\nabla\tilde{\chi}_g \tag{56a}$$

$$\tilde{\kappa} \mathrel{\hat{=}} -\nabla_s\cdot\tilde{\mathbf{n}} \tag{56b}$$

We recall that in our coordinate system $\tilde{\mathbf{n}} = \mathbf{g}_3$.

4.3.2. Transport equation of the filtered sharp-interface

In this section, we are going to express the velocity of the filtered discontinuous interface $\mathbf{v}_{\tilde{\sigma}}$ thanks to the known quantities $\tilde{\chi}_g, \tilde{p}$ and $\tilde{\mathbf{u}}$.

4.3.2.1. Use of the macroscopic variables. The transport equation of the equivalent interface is defined by:

$$\frac{\partial\tilde{\chi}_g}{\partial t} + \mathbf{v}_{\tilde{\sigma}}\cdot\nabla\tilde{\chi}_g = 0 \tag{57}$$

Because the interface is non-material, only the normal velocity is useful, we assume that:

$$\mathbf{v}_{\tilde{\sigma}} = v_{\tilde{\sigma}}\tilde{\mathbf{n}} \tag{58}$$

Because the velocity $\mathbf{v}_{\tilde{\sigma}}$ is the velocity of the local coordinates, one gets:

$$v_{\tilde{\sigma}} \mathrel{\hat{=}} v_3^0 \tag{59}$$

The velocity v_3^0 is given by Eq. (52). Replacing in this Eq. (52) the velocity of the outer regions at order zero, $\bar{\mathbf{u}}^0$, by the velocity of the equivalent discontinuous problem $\tilde{\mathbf{u}}$ (Eq. (54a)), we have:

$$v_{\tilde{\sigma}} = \tilde{\mathbf{u}}\cdot\tilde{\mathbf{n}} - \int_{-\infty}^{+\infty}\frac{D\breve{\tilde{\chi}}_g}{Dt}d\xi + \overline{\tilde{\mathbf{u}}\cdot\tilde{\mathbf{n}}}^{\sigma} - \tilde{\bar{\mathbf{u}}}^{\sigma}\cdot\tilde{\bar{\mathbf{n}}}^{\sigma} \tag{60}$$

The equation above defines the velocity of the equivalent interface with the macroscopic variables. However, the integral term depends on the filtered phase indicator that is a mesoscopic variable. In the following, a closure in term of macroscopic variables is proposed for this term.

4.3.2.2. A closure for the time evolution of the filtered phase indicator. In order to evaluate the time evolution of the filtered phase indicator, we need to specify an interface and a filter. We choose the surface that is described in the following paragraph because it is the simplest one after the plane and the sphere that are supposed to be too bad approximations of an interface that interacts with turbulence. Regarding the filter, we also have to make a choice to have an approximated expression of the filtered phase indicator. The spherical filter is chosen because it is a good estimation of the numerical filter and its isotropy simplifies the algebra. It

is the only time, we need to choose a particular filter for the ISS model.

We note ϕ the angle around the normal. $\phi = 0$ and $\phi = \frac{\pi}{2}$ correspond to the directions of the principal curvatures (Fig. 6). At a given point of the surface bubble, we approximate the interface by a surface whose curvature κ_ϕ is linearly varying with the angle ϕ between the principal curvatures:

$$\kappa_\phi = \frac{1}{R_\phi} = \frac{2}{\pi}(\kappa_2 - \kappa_1)\phi + \kappa_1 \quad \text{for} \quad \phi \in \left[0, \frac{\pi}{2}\right] \tag{61}$$

On $\left[\frac{\pi}{2}, 2\pi\right]$ the curvature is defined by symmetry. Fig. 6 shows examples of such surfaces. Using cylindrical coordinates, a spherical filter and the notations of Fig. 7, the filtered phase indicator $\alpha = \overline{\chi}_g$ is for $z \in [-r, r]$:

$$\alpha(z_f, r, R_1, R_2) = 4\int_{\phi=0}^{\phi=\frac{\pi}{2}} \left(\int_{z=z_f-r}^{z=z_p} \int_{l=0}^{l=\sqrt{r^2-(z-z_f)^2}} l\,dl\,dz + \int_{z=z_p}^{z=0} \int_{l=0}^{l=\sqrt{R_\phi^2-(R_\phi+z)^2}} l\,dl\,dz \right) d\phi \tag{62}$$

After some algebra, one gets for $z \in [-r, r]$:

$$\alpha(z, r, R_1, R_2) = \frac{1}{16r^3}(r-z)^2 \times \left(z + 2r + \frac{3}{z}\left((r+z)^2 \frac{ln\left(1+\frac{z}{R_2}\right) - ln\left(1+\frac{z}{R_1}\right)}{z\left(\frac{1}{R_2}-\frac{1}{R_1}\right)} - r^2 \right) \right) \tag{63}$$

The time derivative of the filtered phase indicator function is expressed thanks to the time evolution of the principal radius as follows:

$$\frac{D\overline{\chi}_g}{Dt} = \frac{DR_1}{Dt}\frac{\partial \overline{\chi}_g}{\partial R_1} + \frac{DR_2}{Dt}\frac{\partial \overline{\chi}_g}{\partial R_2} \tag{64}$$

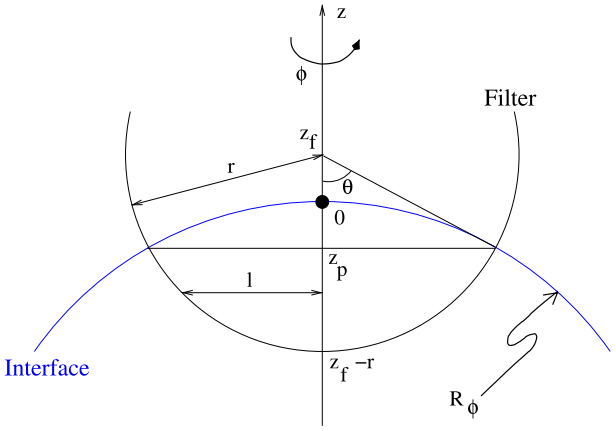

Fig. 7. Geometrical notations.

Using the definition of the mean curvature and Eq. (63), the excess quantity of the time derivative of the filtered phase indicator function becomes:

$$\int_{-r}^{r} \frac{D\overline{\chi}_g}{Dt} d\xi_3 = -\frac{r^2}{10}\frac{D\kappa}{Dt} + HOT \tag{65}$$

Finally, using the time evolution of the mean curvature (Appendix D Eq. (D.19)) and Eqs. (57) and (56a), the transport equation of the filtered discontinuous interface is the following:

$$\frac{\partial \tilde{\chi}_g}{\partial t} = v_{\tilde{\sigma}}\delta_{\tilde{\sigma}} \tag{66a}$$

$$v_{\tilde{\sigma}} = \tilde{\mathbf{u}}\cdot\tilde{\mathbf{n}} + \left(\overline{\tilde{\mathbf{u}}\cdot\tilde{\mathbf{n}}}^{\sigma} - \overline{\tilde{\mathbf{u}}}^{\sigma}\cdot\overline{\tilde{\mathbf{n}}}^{\sigma}\right) + \frac{r^2}{10}(\Delta_s(v_{\tilde{\sigma}}\tilde{\mathbf{n}})\cdot\tilde{\mathbf{n}} + 2\nabla_s(v_{\tilde{\sigma}}\tilde{\mathbf{n}}) : \nabla_s(\tilde{\mathbf{n}})) + HOT \tag{66b}$$

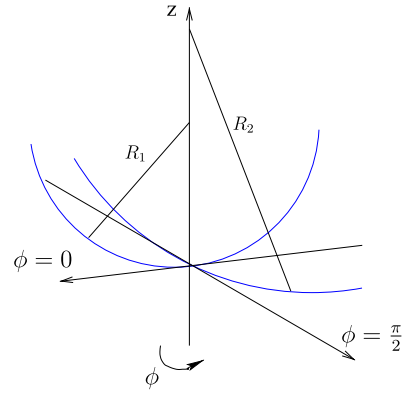

(a) Local cylindrical coordinates

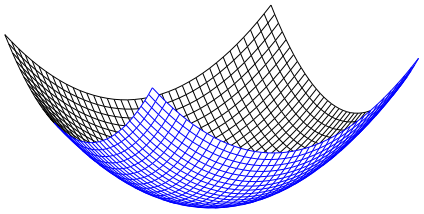

(b) $R_2 = R_1$

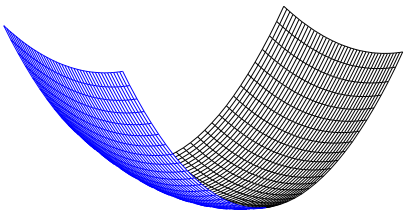

(c) $R_2 = 3R_1$

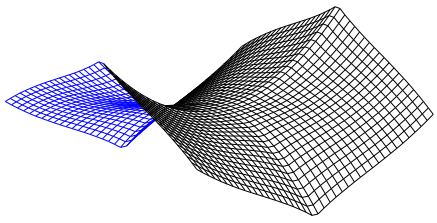

(d) $R_2 = -R_1$

Fig. 6. Anisotropic approximation of a surface ($R_1 = 1$).

This expression is implicit because the time evolution of the filtered discontinuous phase indicator function is known as a function of itself. In *a priori* tests (Toutant et al., accepted for publication), we show that a simple fixed point method is able to correctly evaluate the evolution of the phase indicator function. The term related to the time evolution of the curvature contains a surface Laplacian. In single-phase flow, the Laplacian is used by the techniques of reconstruction (Sagaut, 2003). It allows to estimate the effect of the velocity subgrid fluctuations on the filtered velocity. Here, the surface Laplacian estimate the effect of the velocity subgrid fluctuations on the interface geometry. The coefficients 1 of the correlation between the velocity and the normal and $\frac{r^2}{10}$ of the curvature time evolution depend on the type of the filter (here, a spherical filter has been used). It is necessary to evaluate them again and they are parameters of the closure that we propose. Obviously, the proposed models vanish as the filter size r tends to zero. Last but not least, they are built to respect mass conservation: a bubble keeps its volume until break-up or coalescence occurs. The proposed models modify the bubble shape. Thus the bubble friction surface and its terminal velocity are rectified.

4.3.3. Incompressibility constraint

At order zero, the velocity is continuous across the interface. Consequently, the incompressibility constraint remains the same:

$$\nabla\cdot(\tilde{\mathbf{u}})=0 \tag{67}$$

4.3.4. Momentum equations

Thanks to the matched asymptotic expansions, we have determined the jump conditions of the outer problem at order zero. The particular choice of the filtered discontinuous interface location allows to simplify the surface-excess quantity defined by Eq. (42b). Indeed, using the Lagrangian derivative (Eq. (46)), we have:

$$\begin{aligned}\mathbf{I}_l&=\int_0^{+\infty}\frac{\partial}{\partial t}\left(\breve{\bar{\rho}}\breve{\bar{\mathbf{u}}}^0-\rho_l\bar{\mathbf{u}}_l^0\right)d\xi\\&=\int_0^{+\infty}\left[\frac{D}{Dt}\left(\breve{\bar{\rho}}\breve{\bar{\mathbf{u}}}^0-\rho_l\bar{\mathbf{u}}_l^0\right)-v_3^0\frac{\partial}{\partial\xi}\left(\breve{\bar{\rho}}\breve{\bar{\mathbf{u}}}^0-\rho_l\bar{\mathbf{u}}_l^0\right)\right]d\xi\end{aligned} \tag{68}$$

Since $\breve{\bar{\mathbf{u}}}(\xi_1,\xi_2,\xi)=\bar{\mathbf{u}}(\xi_1,\xi_2,\frac{\xi_3}{\epsilon})$ and since, at order zero, $\breve{\bar{\mathbf{u}}}^0$ does not depend on ξ, one gets:

$$\tilde{\mathbf{u}}=\breve{\bar{\mathbf{u}}}^0=\bar{\mathbf{u}}^0 \tag{69}$$

The integral $\mathbf{I}_l$ becomes:

$$\mathbf{I}_l=\frac{D}{Dt}\left(\tilde{\mathbf{u}}\int_0^{+\infty}\left(\breve{\bar{\rho}}-\rho_l\right)d\xi\right)-v_3^0\tilde{\mathbf{u}}\int_0^{+\infty}\frac{\partial\breve{\bar{\rho}}}{\partial\xi}d\xi \tag{70a}$$

And similarly, we obtain for $\mathbf{I}_g$:

$$\mathbf{I}_g=\frac{D}{Dt}\left(\tilde{\mathbf{u}}\int_{-\infty}^{0}\left(\breve{\bar{\rho}}-\rho_g\right)d\xi\right)-v_3^0\tilde{\mathbf{u}}\int_{-\infty}^{0}\frac{\partial\breve{\bar{\rho}}}{\partial\xi}d\xi \tag{70b}$$

Adding up these integrals, one finds:

$$\mathbf{I}_l+\mathbf{I}_g=\frac{D}{Dt}\left(\tilde{\mathbf{u}}\int_{-\infty}^{+\infty}\left(\breve{\bar{\rho}}-\tilde{\rho}\right)d\xi\right)-v_3^0\tilde{\mathbf{u}}\int_{-\infty}^{+\infty}\frac{\partial\breve{\bar{\rho}}}{\partial\xi}d\xi \tag{70c}$$

The choice of the interface location (Eq. (55)) implies that the excess quantity related to the density is equal to zero:

$$\int_{-\infty}^{+\infty}(\breve{\bar{\rho}}-\tilde{\rho})d\xi=0 \tag{71}$$

By definition of the sharp-interface velocity (Eq. (59)), we have:

$$v_3^0\delta_{\tilde{\sigma}}=\frac{\partial\tilde{\chi}_g}{\partial t}=-\frac{\partial\tilde{\chi}_l}{\partial t} \tag{72}$$

Finally, noting that $\int_{-\infty}^{+\infty}\frac{\partial\bar{\rho}}{\partial\xi}d\xi=\rho_l-\rho_g$, it comes:

$$\delta_{\tilde{\sigma}}(\mathbf{I}_l+\mathbf{I}_g)=\sum_k\rho_k\tilde{\mathbf{u}}_k\frac{\partial\tilde{\chi}_k}{\partial t} \tag{73}$$

Thanks to this new writing and according to the definition (54b), the momentum jump condition (Eq. (41)) is at order zero:

$$\begin{aligned}&\sum_k\left(\rho_k\tilde{\mathbf{u}}_k\frac{\partial\tilde{\chi}_k}{\partial t}+(\widetilde{p_k}\mathbf{I}-\widetilde{\mathbf{S}_k}+\rho_k(\widetilde{\mathbf{u}_k}\otimes\widetilde{\mathbf{u}_k}-\widetilde{\mathscr{L}_k}))\cdot\nabla\tilde{\chi}_k\right)\\&\quad=\left(\sigma\tilde{\kappa}\tilde{\mathbf{n}}-\int_{-r}^{+r}\frac{\partial(\overline{\bar{\rho}\bar{\mathbf{u}}}-\bar{\bar{\rho}}\bar{\bar{\mathbf{u}}})}{\partial t}d\xi_3\right)\delta_{\tilde{\sigma}}\end{aligned} \tag{74}$$

In this equation, we recover the DNS jump conditions corrected by a model that takes into account the subgrid interaction between interface and turbulence. With the proposed model, the integral of the time evolution of the correlations between density and velocity is added to the capillary forces. Contrary to the capillary forces this term has a non-zero contribution in the tangential directions. Indeed, at the macroscopic level, the transfers of kinetic energy across the interface are underestimated. The tangential contribution allows to correct this defect.

4.3.5. System of discontinuous filtered equation

We have established the following system of equations

- incompressibility constraint:

$$\nabla\cdot(\tilde{\mathbf{u}})=0 \tag{75a}$$

- filtered discontinuous interface transport:

$$\begin{aligned}&\frac{\partial\tilde{\chi}_g}{\partial t}=v_{\tilde{\sigma}}\delta_{\tilde{\sigma}}\\&v_{\tilde{\sigma}}=\tilde{\mathbf{u}}\cdot\tilde{\mathbf{n}}+\underbrace{(\overline{\tilde{\mathbf{u}}\cdot\tilde{\mathbf{n}}}^{\sigma}-\bar{\tilde{\mathbf{u}}}^{\sigma}\cdot\bar{\tilde{\mathbf{n}}}^{\sigma})}_{\mathrm{I}}+\underbrace{\frac{r^2}{10}(\Delta_s(v_{\tilde{\sigma}}\tilde{\mathbf{n}})\cdot\tilde{\mathbf{n}}+2\nabla_s(v_{\tilde{\sigma}}\tilde{\mathbf{n}}):\nabla_s(\tilde{\mathbf{n}}))}_{\mathrm{II}}\end{aligned} \tag{75b}$$

- momentum balance equation:

$$\begin{aligned}\frac{\partial\tilde{\rho}\tilde{\mathbf{u}}}{\partial t}+\nabla\cdot(\tilde{\rho}\tilde{\mathbf{u}}\otimes\tilde{\mathbf{u}})&=-\nabla\tilde{p}+\nabla\cdot(\widetilde{\mathbf{S}})+\nabla\cdot(\tilde{\rho}\widetilde{\mathscr{L}})\\&\quad+\left(\sigma\tilde{\kappa}\tilde{\mathbf{n}}-\int_{-\infty}^{+\infty}\underbrace{\frac{\partial(\overline{\bar{\rho}\bar{\mathbf{u}}}-\bar{\bar{\rho}}\bar{\bar{\mathbf{u}}})}{\partial t}}_{\mathrm{III}}d\xi_3\right)\delta_{\tilde{\sigma}}\end{aligned} \tag{75c}$$

When the filter size tends to zero, these equations tend naturally toward the DNS equations. Indeed, the terms specific to ISS are weighted by r^2 or are correlations.

In Eqs. (75b) and (75c), the terms denoted I and III correspond to a kind of interfacial scale similarity hypothesis. These terms are actually consequences of the scale similarity hypothesis used to model τ_{interf} and τ_{temp} (*cf.* Eqs. (10a) and (10b)) at the mesoscopic scale. The term denoted II in Eq. (75b) is not related to the assumption made to close the model at the mesoscopic scale and will appear whatever the mesoscopic model because we remind that it comes from the time evolution of the mean interface curvature (*cf.* Appendix D). However, the methodology presented using the method of matched asymptotic expansions could be used as it is using another closure model at the mesoscopic scale instead of the scale similarity hypothesis. Corresponding jump conditions would be obtained in which excess quantities corresponding to the terms I and III of the present model would depend on this other closure model. Thus, we believe that the methodology presented is

general in the sense that it is not associated to a particular form of the closure used at the mesoscopic scale.

5. Conclusions and perspectives

We propose an original method to define mathematically a discontinuous filtered interface. It consists in applying a centered filter all over the domain and thus possibly crossed by an interface. This operation smears out the interface that thus becomes a continuous transition zone. Then, we make this transition zone tends toward an equivalent discontinuity. This explicit filtering approach mimics the implicit filter of numerical methods that deal with discontinuous interfaces. Moreover, this approach enables us to determine the jump conditions of the filtered quantities. We find that, like DNS, the velocity is continuous across the interface and that, unlike DNS, the jump conditions related to the momentum equation cannot be modeled by the sole surface tension. Indeed, the excess quantity of the density-velocity correlation has to be added to the capillary force to accurately account for the subgrid kinetic energy transfers across the interface. Unlike the capillary force, this new force has components tangential to the interface. Furthermore, we show that the filtered discontinuous interface cannot be moved by simply using the filtered fluid velocity. Two additional terms appear in the expression for the interface velocity: a surface scale similarity term that takes into account the correlation between the velocity and the normal to the interface and the time evolution of the curvature that takes into account the effect of the velocity subgrid fluctuations on the interface geometry. Finally, using these new jump conditions, we determine the one-fluid equations for filtered quantities.

In the part 2, we realize a DNS of a fully deformable bubble interacting with a grid turbulence to validate the proposed jump conditions thanks to *a priori* tests (Toutant et al., accepted for publication).

Current investigations deal with the implementation of the proposed models. Their accuracy and the gain that they allow compared to DNS are investigated thanks to *a posteriori* tests.

Acknowledgments

The authors want to thank E. Labourasse, P. Sagaut and O. Simonin for useful discussions. The authors also want to thank G. Bois who has read very carefully the paper and has participated to its improvement.

Appendix A. Local orthogonal curvilinear coordinates

Let (ξ_1,ξ_2,ξ_3) be the local curvilinear coordinates related to the ISS filtered discontinuous interface. (ξ_1,ξ_2) are the surface coordinates and ξ_3 the normal coordinate. At each point M, we have

$$\mathbf{OM} = \mathbf{r}_0(\xi_1,\xi_2) + \xi_3\tilde{\mathbf{n}} \tag{A.1}$$

where $\tilde{\mathbf{n}}$ is the unit normal to the ISS filtered discontinuous interface (Anderson et al., 2001; Garrigues, 1999; Aris, 1962). Let us note $(\mathbf{t}_1,\mathbf{t}_2)$ the unit tangent vectors related to the principal curvatures. These two directions are orthogonal (Garrigues, 1999). The natural basis $\{\mathbf{g}_i\}$ associated to these coordinates is defined by:

$$\mathbf{g}_i = \frac{\partial \mathbf{OM}}{\partial \xi_i} \tag{A.2}$$

We have

$$\mathbf{g}_1 = (1-\xi_3\kappa_1)\mathbf{t}_1, \quad \mathbf{g}_2 = (1-\xi_3\kappa_2)\mathbf{t}_2, \quad \mathbf{g}_3 = \tilde{\mathbf{n}} \tag{A.3}$$

where κ_1 and κ_2 are the principal curvatures of the surface $\xi_3 = 0$ (Anderson et al., 2001; Garrigues, 1999). Let $\mathbf{V}$ be a vector, one gets $\mathbf{V} = V^i\,\mathbf{g}_i$. The components V^i are called *contravariant components* of $\mathbf{V}$. The reciprocal basis $\{\mathbf{g}^i\}$ is defined by

$$\mathbf{g}_i \cdot \mathbf{g}^j = \delta_i^j \tag{A.4}$$

where δ_i^j is equal to 1 if $i=j$ and to 0 otherwise. We can write $\mathbf{V} = V_i\,\mathbf{g}^i$ and the components V_i are called *covariant components* of $\mathbf{V}$. The metric tensor is defined by:

$$g_{ij} = \mathbf{g}_i \cdot \mathbf{g}_j \tag{A.5}$$

The scale factors are:

$$h_i = \sqrt{g_{ii}} \tag{A.6}$$

In our case, they can be written as follows:

$$h_1 = |1-\xi_3\kappa_1|, \quad h_2 = |1-\xi_3\kappa_2|, \quad h_3 = 1 \tag{A.7}$$

Unfortunately, the natural basis is not normalized. In order to avoid this drawback, we introduce the normalized natural basis also called physical basis:

$$\left\{\tilde{\mathbf{g}}_i = \frac{\mathbf{g}_i}{\|\mathbf{g}_i\|} = \frac{\mathbf{g}_i}{h_i} = \frac{\mathbf{g}^i}{\|\mathbf{g}^i\|} = \mathbf{g}^i h_i\right\} = (\mathbf{t}_1,\mathbf{t}_2,\tilde{\mathbf{n}}) \tag{A.8}$$

We use the *physical components* of vectors that verify:

$$\mathbf{u} = u(i)\tilde{\mathbf{g}}_i, \quad \text{with} \quad u(i) = h_i u^i = \frac{u_i}{h_i} \tag{A.9}$$

A.1. Normal curvature tensor

The covariant components of the normal curvature tensor, $\mathbf{B}$, are defined by:

$$b_{\alpha\beta} = \tilde{\mathbf{n}} \cdot \frac{\partial \mathbf{t}_\alpha}{\partial \xi_\beta} = -\mathbf{t}_\alpha \cdot \frac{\partial \tilde{\mathbf{n}}}{\partial \xi_\beta} \tag{A.10}$$

Thus, one has:

$$\mathbf{B} = -\nabla_s \tilde{\mathbf{n}} \tag{A.11}$$

where ∇_s is the surface gradient. Let us note the eigen values of $\mathbf{B}$ (*i.e.* the principal curvatures) $\kappa_1 = 1/R_1$ and $\kappa_2 = 1/R_2$. One defines:

- the mean curvature, $\kappa = Tr\mathbf{B} = 1/R_1 + 1/R_2$,
- the Gaussian curvature, $H = det\mathbf{B} = 1/(R_1R_2)$.

A.2. Normal components of the shear stress

The spatial derivative of the velocity along the normal direction is

$$\tilde{\mathbf{n}} \cdot \nabla \mathbf{u} = u^j_{,3}\mathbf{g}_j + u^1\Gamma^1_{13}\mathbf{g}_1 + u^2\Gamma^2_{23}\mathbf{g}_2 \tag{A.12}$$

where Γ^k_{ij} are the Christoffel coefficients (Garrigues, 2001) defined by:

$$\frac{\partial \mathbf{g}_i}{\partial \xi_j} = \Gamma^k_{ij}\mathbf{g}_k \tag{A.13}$$

In the orthonormal physical basis, one simply has:

$$\tilde{\mathbf{n}} \cdot \nabla \mathbf{u} = u(j)_{,3}\tilde{\mathbf{g}}_j \tag{A.14}$$

Finally, the normal components of the shear stress can be written as follows:

$$\tilde{\mathbf{n}}\cdot(\nabla\mathbf{u}+\nabla^T\mathbf{u}) = \left(u(1)_{,3}+\frac{u(3)_{,1}+u(1)\kappa_1}{h_1}\right)\tilde{\mathbf{g}}_1 + \left(u(2)_{,3}+\frac{u(3)_{,2}+u(2)\kappa_2}{h_2}\right)\tilde{\mathbf{g}}_2 + 2u(3)_{,3}\tilde{\mathbf{g}}_3 \quad (A.15)$$

A.3. Divergence of the shear stress

Let us note:

$$\mathbf{S} = \mu(\nabla\mathbf{u}+\nabla^T\mathbf{u}) \quad (A.16)$$

The divergence of this tensor (Garrigues, 2001, Chap. 2) is:

$$(\nabla\cdot\mathbf{S})_i = (\nabla\mathbf{S})_{ikk} = S_{ik,k} - S_{mk}\Gamma^m_{ki} - S_{im}\Gamma^m_{kk} \quad (A.17)$$

At order 1 of the normal coordinates ξ_3, we find:

$$\begin{aligned}(\nabla\cdot\mathbf{S})_1 &= 2(\mu u(1)_{,1})_{,1} + (\mu u(1)_{,2})_{,2} + (\mu u(2)_{,1})_{,2} + (\mu u(1)_{,3})_{,3}\\ &+ (\mu u(3)_{,1})_{,3} + \kappa_1((\mu u(1))_{,3} - \mu u(1)_{,3}\\ &- 2\mu u(3)_{,1} - \xi_3(\mu u(1)_{,3})_{,3}) - \mu(\kappa_1+\kappa_2)(u(3)_{,1}\\ &+ u(1)_{,3} + \kappa_1 u(1) - \xi_3\kappa_2 u(1)_{,3})\\ &+ 4\mu\kappa_1^2\xi_3 u(1)_{,3} - 2\mu\kappa_{1,1}u(3) + \mathcal{O}(\xi_3) \quad (A.18a)\end{aligned}$$

$$\begin{aligned}(\nabla\cdot\mathbf{S})_2 &= 2(\mu u(2)_{,2})_{,2} + (\mu u(1)_{,2})_{,2} + (\mu u(2)_{,1})_{,2}\\ &+ (\mu u(2)_{,3})_{,3} + (\mu u(3)_{,2})_{,3} + \kappa_2((\mu u(2))_{,3}\\ &- \mu u(2)_{,3} - 2\mu u(3)_{,2} - \xi_3(\mu u(2)_{,3})_{,3})\\ &- \mu(\kappa_1+\kappa_2)(u(3)_{,2} + u(1)_{,3} + \kappa_2 u(2) - \xi_3\kappa_1 u(2)_{,3})\\ &+ 4\mu\kappa_2^2\xi_3 u(2)_{,3} - 2\mu\kappa_{2,2}u(3) + \mathcal{O}(\xi_3) \quad (A.18b)\end{aligned}$$

$$\begin{aligned}(\nabla\cdot\mathbf{S})_3 &= 2(\mu u(3)_{,3})_{,3} + (\mu u(1)_{,3})_{,1} + (\mu u(3)_{,1})_{,1}\\ &+ (\mu u(2)_{,3})_{,2} + (\mu u(3)_{,2})_{,2} + \kappa_1((\mu u(1))_{,1}\\ &- 2\mu u(3)_{,3} - \xi_3(\mu u(1)_{,3})_{,1} - \mu u(3)\kappa_1)\\ &+ \kappa_2((\mu u(2))_{,2} - 2\mu u(3)_{,3} - \xi_3(\mu u(2)_{,3})_{,2}\\ &- \mu u(3)\kappa_2) + \mu\xi_3((\kappa_{1,1}-\kappa_{2,2})(u(1)_{,3}-u(2)_{,3})\\ &+ 2u(3)_{,3}(\kappa_1+\kappa_2)) + \mathcal{O}(\xi_3) \quad (A.18c)\end{aligned}$$

Appendix B. Property of the mesoscopic models

In this section, we prove that the integrals over the interfacial transition region of the mesoscopic models and of the validated expressions are equal at order zero:

$$\int\left(\tau^{meso}_{interf} - \tau^{ve}_{interf}\right)d\xi_3 = 0 \quad (B.1a)$$

$$\int\left(\boldsymbol{\tau}^{meso}_{temp} - \boldsymbol{\tau}^{ve}_{temp}\right)d\xi_3 = 0 \quad (B.1b)$$

$$\int(\boldsymbol{\tau}^{meso}_{conv} - \boldsymbol{\tau}^{ve}_{conv})d\xi_3 = 0 \quad (B.1c)$$

The coordinate ξ_3 is associated to the direction normal to the interface (see Appendix A). The order zero is the lowest order introduced by the method of matched asymptotic expansions (see Section 4.2.2). At this order, we show in Section 4.2.4.1 that the velocity is independent of ξ_3. [4] Consequently, the only variation along ξ_3 is due to the density that is constant within the bulk phases. Thus, it is equivalent to prove that

$$\int(\overline{\chi f} - \overline{\chi}\,\overline{f})d\xi_3 = 0 \quad (B.2)$$

where f is a function independent of ξ_3. We remind that the filtering operation, $\bar{\cdot}$, is defined by:

$$\bar{\phi}(x^0) = \int G(x^0 - x)\,\phi(x)\,dx \quad (B.3)$$

It is worth noting that the $\bar{\phi}$ can also be written as follows:

$$\bar{\phi}(x^0) = \int G(x)\,\phi(x^0 - x)\,dx \quad (B.4)$$

Thus, one gets:

$$\begin{aligned}\int(\overline{\chi f} - \overline{\chi}\,\overline{f})d\xi_3 &= \int\overline{(\chi-\bar{\chi})f}\,d\xi_3 = \int_{\xi_3}\left[\int_{\xi_i^0}\int_{\xi_3^0}(\chi(\xi_i-\xi_i^0,\xi_3-\xi_3^0)\right.\\ &\left.-\bar{\chi}(\xi_i-\xi_i^0,\xi_3-\xi_3^0))f(\xi_i-\xi_i^0)G(\xi_i^0,\xi_3^0)dV^0\right]d\xi_3\int_{\xi_i^0}\\ &\times\int_{\xi_3^0}\left[\int_{\xi_3}(\chi(\xi_i-\xi_i^0,\xi_3-\xi_3^0)-\bar{\chi}(\xi_i-\xi_i^0,\xi_3-\xi_3^0))d\xi_3\right]\\ &\times f(\xi_i-\xi_i^0)G(\xi_i^0,\xi_3^0)dV^0 \approx 0 \quad (B.5)\end{aligned}$$

To obtain this result, we use the fact that, at order zero in ϵ, we have:

$$\int_{\xi_3}(\chi-\bar{\chi})d\xi_3 \approx 0$$

We can prove this property using the local mass conservation:

$$\int_V(\chi-\bar{\chi})dV = 0$$

Indeed, at order zero in ϵ, the integral over the volume could be reduced to an integral along the normal direction:

$$\begin{aligned}\int_V(\chi-\bar{\chi})dV &= \int_{\xi_1,\xi_2,\xi_3}(\chi-\bar{\chi})\,|1-\xi_3\kappa_1||1-\xi_3\kappa_2|\,d\xi_1d\xi_2d\xi_3\\ &= \int_{\xi_1,\xi_2,\xi}(\chi-\bar{\chi})\,|1-\epsilon\xi\kappa_1||1-\epsilon\xi\kappa_2|\,d\xi_1d\xi_2d\xi\\ &\approx \int_{\xi_1,\xi_2,\xi}(\chi-\bar{\chi})\,d\xi_1d\xi_2d\xi = \int_{\xi_1,\xi_2}d\xi_1d\xi_2\int_{\xi}(\chi-\bar{\chi})\,d\xi\\ &= \int_{\xi_1,\xi_2}d\xi_1d\xi_2\int_{\xi_3}(\chi-\bar{\chi})\,d\xi_3 \quad (B.6)\end{aligned}$$

The equality between the third and the fourth line is due to the fact that the domain of the integral along the tangential coordinates ξ_1 and ξ_2 is arbitrary. Thus, one can choose it as small as necessary to verify that χ and $\bar{\chi}$ do not depend on ξ_1 and ξ_2.

Appendix C. Tensor jump conditions

In this appendix, we detail the calculus that determines the interface jump condition of the momentum. Integrating the subtraction between Eqs. (40) related to the order 1 of momentum in the inner region and Eq. (33b) related to the order zero in the outer region, one gets

$$\begin{aligned}&\lim_{\xi\to+\infty}\left(\breve{\mu}\breve{u}^1(1)_{,3} + \breve{\mu}\breve{u}^0(3)_{,1} + \kappa_1\left(\breve{\mu}\breve{u}^0(1)\right)\right)\\ &- \lim_{\xi\to-\infty}\left(\breve{\mu}\breve{u}^1(1)_{,3} + \breve{\mu}\breve{u}^0(3)_{,1} + \kappa_1\left(\breve{\mu}\breve{u}^0(1)\right)\right)\\ &= I_l(1) + I_g(1) + \int_{-\infty}^{+\infty}\frac{\partial\breve{T}^0}{\partial t}(1)d\xi + \lim_{\xi\to+\infty}\left(\breve{\rho}\breve{u}^0(1)\breve{u}^0(3) + \breve{C}^0_{13}\right)\\ &- \lim_{\xi\to-\infty}\left(\breve{\rho}\breve{u}^0(1)\breve{u}^0(3) + \breve{C}^0_{13}\right) \quad (C.1a)\end{aligned}$$

[4] In this paper, we only study the order zero. Thus, the equality of the integrals at this order is enough to validate the models.

$$\lim_{\xi\to+\infty}\left(\breve{\bar{\mu}}\breve{\bar{u}}^1(2)_{,3}+\breve{\bar{\mu}}\breve{\bar{u}}^0(3)_{,2}+\kappa_2\left(\breve{\bar{\mu}}\breve{\bar{u}}^0(2)\right)\right)$$
$$-\lim_{\xi\to-\infty}\left(\breve{\bar{\mu}}\breve{\bar{u}}^1(2)_{,3}+\breve{\bar{\mu}}\breve{\bar{u}}^0(3)_{,2}+\kappa_2\left(\breve{\bar{\mu}}\breve{\bar{u}}^0(2)\right)\right)$$
$$=I_l(2)+I_g(2)+\int_{-\infty}^{+\infty}\frac{\partial\breve{\bar{T}}^0}{\partial t}(2)d\xi+\lim_{\xi\to+\infty}\left(\breve{\bar{\rho}}\breve{\bar{u}}^0(2)\breve{\bar{u}}^0(3)+\breve{C}^0_{23}\right)$$
$$-\lim_{\xi\to-\infty}\left(\breve{\bar{\rho}}\breve{\bar{u}}^0(2)\breve{\bar{u}}^0(3)+\breve{C}^0_{23}\right) \tag{C.1b}$$

$$\lim_{\xi\to+\infty}\left(2\left(\breve{\bar{\mu}}\breve{\bar{u}}^1(3)_{,3}\right)-\breve{\bar{p}}^0\right)-\lim_{\xi\to-\infty}\left(2\left(\breve{\bar{\mu}}\breve{\bar{u}}^1(3)_{,3}\right)-\breve{\bar{p}}^0\right)\sigma\int_{-\infty}^{+\infty}\breve{\kappa}^0_{\breve{\chi}}\breve{\chi}_{g,3}d\xi$$
$$=I_l(3)+I_g(3)+\int_{-\infty}^{+\infty}\frac{\partial\breve{\bar{T}}^0}{\partial t}(3)d\xi+\lim_{\xi\to+\infty}\left(\breve{\bar{\rho}}\breve{\bar{u}}^0(3)\breve{\bar{u}}^0(3)+\breve{C}^0_{33}\right)$$
$$-\lim_{\xi\to-\infty}\left(\breve{\bar{\rho}}\breve{\bar{u}}^0(3)\breve{\bar{u}}^0(3)+\breve{C}^0_{33}\right) \tag{C.1c}$$

where $\mathbf{I}_l$ and $\mathbf{I}_g$ are defined by:

$$\mathbf{I}_l=\int_0^{+\infty}\frac{\partial}{\partial t}\left(\breve{\bar{\rho}}\breve{\bar{\mathbf{u}}}^0-\rho_l\bar{\mathbf{u}}^0_l\right)d\xi \tag{C.2a}$$

$$\mathbf{I}_g=\int_{-\infty}^{0}\frac{\partial}{\partial t}\left(\breve{\bar{\rho}}\breve{\bar{\mathbf{u}}}^0-\rho_g\bar{\mathbf{u}}^0_g\right)d\xi \tag{C.2b}$$

These integrals represent respectively the time evolution of the subtraction between microscopic (related to the inner region) and macroscopic (related to the outer region) momentum on the liquid and gas sides.

Using the matching conditions (35a) and (35c), Eq. (C.1a) reduce to:

$$\left(\bar{\mu}\bar{u}^0(1)_{,3}+\bar{\mu}\bar{u}^0(3)_{,1}+\kappa_1\left(\bar{\mu}\bar{u}^0(1)\right)\right)\Big|_+$$
$$-\left(\bar{\mu}\bar{u}^0(1)_{,3}+\bar{\mu}\bar{u}^0(3)_{,1}+\kappa_1\left(\bar{\mu}\bar{u}^0(1)\right)\right)\Big|_-$$
$$=I_l(1)+I_g(1)+\int_{-\infty}^{+\infty}\frac{\partial\breve{\bar{T}}^0}{\partial t}(1)d\xi+\left(\bar{\rho}\bar{u}^0(1)\bar{u}^0(3)+C^0_{13}\right)\Big|_+$$
$$-\left(\bar{\rho}\bar{u}^0(1)\bar{u}^0(3)+C^0_{13}\right)\Big|_- \tag{C.3a}$$

$$\left(\bar{\mu}\bar{u}^0(2)_{,3}+\bar{\mu}\bar{u}^0(3)_{,2}+\kappa_2\left(\bar{\mu}\bar{u}^0(2)\right)\right)\Big|_+$$
$$-\left(\bar{\mu}\bar{u}^0(2)_{,3}+\bar{\mu}\bar{u}^0(3)_{,2}+\kappa_2\left(\bar{\mu}\bar{u}^0(2)\right)\right)\Big|_-=I_l(2)+I_g(2)$$
$$+\int_{-\infty}^{+\infty}\frac{\partial\breve{\bar{T}}^0}{\partial t}(2)d\xi+\left(\bar{\rho}\bar{u}^0(2)\bar{u}^0(3)+C^0_{23}\right)\Big|_+-\left(\bar{\rho}\bar{u}^0(2)\bar{u}^0(3)+C^0_{23}\right)\Big|_- \tag{C.3b}$$

$$\left(2\left(\bar{\mu}\bar{u}^0(3)_{,3}\right)-\bar{p}^0\right)\Big|_+-\left(2\left(\bar{\mu}\bar{u}^0(3)_{,3}\right)-\bar{p}^0\right)\Big|_--\sigma\int_{-\infty}^{+\infty}\breve{\kappa}^0_{\breve{\chi}}\breve{\chi}_{g,3}d\xi$$
$$=I_l(3)+I_g(3)+\int_{-\infty}^{+\infty}\frac{\partial\breve{\bar{T}}^0}{\partial t}(3)d\xi+\left(\bar{\rho}\bar{u}^0(3)\bar{u}^0(3)+C^0_{33}\right)\Big|_+$$
$$-\left(\bar{\rho}\bar{u}^0(3)\bar{u}^0(3)+C^0_{33}\right)\Big|_- \tag{C.3c}$$

Because when $\xi_3=0$, we get $h_1=h_2=1$ (Appendix A), the jump of the terms involving viscosity in the previous equations are exactly the shear stress jump along the normal direction (Eq. (A.15) Appendix A).

Regarding the term related to the capillary force, at order zero, one gets:

$$\breve{\mathbf{n}}_{\breve{\chi}}(\xi_1,\xi_2,\xi)=\tilde{\mathbf{n}}(\xi_1,\xi_2) \tag{C.4}$$

where $\tilde{\mathbf{n}}$ is the normal to the ISS filtered discontinuous interface. Thus, at order zero, it comes:

$$\breve{\kappa}^0_{\breve{\chi}}(\xi_1,\xi_2,\xi)=\tilde{\kappa}(\xi_1,\xi_2) \tag{C.5}$$

where $\tilde{\kappa}$ is the curvature associated to the ISS filtered discontinuous interface. Using this equation and the matching condition (34), the term related to the capillary force becomes:

$$\sigma\int_{-\infty}^{+\infty}\breve{\kappa}^0_{\breve{\chi}}\breve{\chi}_{g,3}d\xi=\sigma\tilde{\kappa}\int_{-\infty}^{+\infty}\frac{\partial\breve{\chi}_g}{\partial\xi}d\xi=\sigma\tilde{\kappa}(\chi_g|_+-\chi_g|_-)=-\sigma\tilde{\kappa} \tag{C.6}$$

Thus, Eq. (C.3c) becomes:

$$\left(2\left(\bar{\mu}\bar{u}^0(3)_{,3}\right)-\bar{p}^0\right)\Big|_+-\left(2\left(\bar{\mu}\bar{u}^0(3)_{,3}\right)-\bar{p}^0\right)\Big|_-+\sigma\tilde{\kappa}$$
$$=I_l(3)+I_g(3)+\int_{-\infty}^{+\infty}\frac{\partial\breve{\bar{T}}^0}{\partial t}(3)d\xi+\left(\bar{\rho}\bar{u}^0(3)\bar{u}^0(3)+C^0_{33}\right)\Big|_+$$
$$-\left(\bar{\rho}\bar{u}^0(3)\bar{u}^0(3)+C^0_{33}\right)\Big|_-$$

In this relation, we recover the momentum jump condition of DNS with the surface tension corrected by the integral quantity of the subgrid term related to acceleration $I_l(3)+I_g(3)+\int_{-\infty}^{+\infty}\frac{\partial\breve{\bar{T}}^0}{\partial t}(3)d\xi$. This integral quantity is a new force similar to the capillary force. However, whereas the capillary force has only a normal component, this subgrid term may get tangential components.

The momentum jump conditions (Eqs. (C.3a), (C.3b) and (C.7)) can be rewritten in only one equation:

$$\left(\left(\bar{\mathbf{S}}^0-\bar{p}^0\mathbf{I}\right)\big|_+-\left(\bar{\mathbf{S}}^0-\bar{p}^0\mathbf{I}\right)\big|_-\right)\cdot\tilde{\mathbf{n}}+\sigma\tilde{\kappa}\tilde{\mathbf{n}}$$
$$=\mathbf{I}_l+\mathbf{I}_g+\int_{-\infty}^{+\infty}\frac{\partial\breve{\bar{\mathbf{T}}}^0}{\partial t}d\xi+\left(\left(\bar{\rho}\bar{\mathbf{u}}^0\otimes\bar{\mathbf{u}}^0+\mathbf{C}^0\right)\Big|_+-\left(\bar{\rho}\bar{\mathbf{u}}^0\otimes\bar{\mathbf{u}}^0+\mathbf{C}^0\right)\Big|_-\right)\cdot\tilde{\mathbf{n}} \tag{C.8}$$

In this relation, the momentum jump conditions of DNS are corrected by the integral quantity of the subgrid terms related to acceleration $\mathbf{I}_l+\mathbf{I}_g+\int_{-\infty}^{+\infty}\frac{\partial\breve{\bar{\mathbf{T}}}^0}{\partial t}d\xi$.

Appendix D. Time evolution of principal curvatures

The time evolution of the mean curvature presented in *Theory of Multicomponent Fluids* (Drew and Passman, 1999, chap. 17.2.1) depends on the Laplacian of the velocity instead of the surface Laplacian. This is the reason why we propose a new proof.

The interface is defined by the vector function $\mathbf{x}$

$$\mathbf{x}:\quad \mathbb{R}^2\times\mathbb{R}^+\to\mathbb{R}^3$$
$$(\xi_1,\xi_2,t)\mapsto\mathbf{x}(\xi_1,\xi_2,t) \tag{D.1}$$

where (ξ_1,ξ_2) are the surface coordinates and t the time. By definition, the interface velocity is:

$$\mathbf{v}(\xi_1,\xi_2,t)=\frac{\partial\mathbf{x}}{\partial t} \tag{D.2}$$

The time derivative of this section is a Lagrangian derivative because we follow the interface. Because the interface is non-material, we can assume that

$$\mathbf{v}(\xi_1,\xi_2,t)=v(\xi_1,\xi_2,t)\mathbf{n}(\xi_1,\xi_2,t) \tag{D.3}$$

where $\mathbf{n}$ is the normal to the interface. Furthermore, we assume that the local coordinates are such that each point $\mathbf{x}$ on the interface corresponding to the surface coordinates (ξ_1,ξ_2) is moving along the normal direction. Thus, we assume that both the surface and the surface coordinates are moving along the normal direction.

Let $\mathbf{t}_\alpha(\alpha = 1\text{or}2)$ be the orthogonal basis related to the principal curvatures. If $\xi_3 = 0$, we have:

$$\frac{\partial \mathbf{x}}{\partial \xi_\alpha} = \mathbf{t}_\alpha \tag{D.4a}$$

$$\frac{\partial \mathbf{n}}{\partial \xi_\alpha} = -\frac{1}{R_\alpha}\mathbf{t}_\alpha \tag{D.4b}$$

$$\frac{\partial \mathbf{t}_\alpha}{\partial \xi_\alpha} = \frac{1}{R_\alpha}\mathbf{n} \tag{D.4c}$$

Using (D.4a) and (D.4b), one finds

$$\frac{\partial \mathbf{x}}{\partial \xi_\alpha} = -R_\alpha \frac{\partial \mathbf{n}}{\partial \xi_\alpha} \tag{D.5}$$

where $R_\alpha = \frac{1}{\kappa_\alpha}$, $\alpha = 1, 2$ are the principal radii of curvature. The time derivative of (D.5) gives for the left hand side

$$\frac{\partial}{\partial t}\frac{\partial \mathbf{x}}{\partial \xi_\alpha} = \frac{\partial}{\partial \xi_\alpha}\frac{\partial \mathbf{x}}{\partial t} = \frac{\partial \mathbf{v}}{\partial \xi_\alpha} = \frac{\partial v}{\partial \xi_\alpha}\mathbf{n} + v\frac{\partial \mathbf{n}}{\partial \xi_\alpha}, \tag{D.6a}$$

and for the right hand side

$$\frac{\partial}{\partial t}\left(-R_\alpha \frac{\partial \mathbf{n}}{\partial \xi_\alpha}\right) = -\frac{\partial R_\alpha}{\partial t}\frac{\partial \mathbf{n}}{\partial \xi_\alpha} - R_\alpha \frac{\partial}{\partial t}\frac{\partial \mathbf{n}}{\partial \xi_\alpha}, \tag{D.6b}$$

Thus, we have:

$$-\frac{\partial R_\alpha}{\partial t}\frac{\partial \mathbf{n}}{\partial \xi_\alpha} - R_\alpha \frac{\partial}{\partial t}\frac{\partial \mathbf{n}}{\partial \xi_\alpha} = \frac{\partial v}{\partial \xi_\alpha}\mathbf{n} + v\frac{\partial \mathbf{n}}{\partial \xi_\alpha} \tag{D.6c}$$

The fact that $\mathbf{n}\cdot\mathbf{n} = 1$ implies:

$$\frac{\partial \mathbf{n}}{\partial \xi_\alpha}\cdot\mathbf{n} = 0 \tag{D.7a}$$

$$\frac{\partial \mathbf{n}}{\partial t}\cdot\mathbf{n} = 0 \tag{D.7b}$$

The scalar product of $\frac{\partial \mathbf{n}}{\partial \xi_\alpha}$ and (D.6c) gives:

$$\frac{\partial R_\alpha}{\partial t} = -v - R_\alpha \frac{\frac{\partial \mathbf{n}}{\partial \xi_\alpha}\cdot\frac{\partial}{\partial \xi_\alpha}\frac{\partial \mathbf{n}}{\partial t}}{\frac{\partial \mathbf{n}}{\partial \xi_\alpha}\cdot\frac{\partial \mathbf{n}}{\partial \xi_\alpha}} \tag{D.8}$$

Using (D.4b) and (D.4c), we can write:

$$\begin{aligned}
\frac{\partial \mathbf{n}}{\partial \xi_\alpha}\cdot\frac{\partial \mathbf{n}}{\partial \xi_\alpha} &= \frac{1}{R_\alpha^2}\\
\frac{\partial \mathbf{n}}{\partial \xi_\alpha}\cdot\frac{\partial}{\partial \xi_\alpha}\frac{\partial \mathbf{n}}{\partial t} &= -\frac{1}{R_\alpha}\mathbf{t}_\alpha\cdot\frac{\partial}{\partial \xi_\alpha}\frac{\partial \mathbf{n}}{\partial t}\\
&= -\frac{1}{R_\alpha}\left(\frac{\partial}{\partial \xi_\alpha}\left(\mathbf{t}_\alpha\cdot\frac{\partial \mathbf{n}}{\partial t}\right) - \frac{\partial \mathbf{t}_\alpha}{\partial \xi_\alpha}\cdot\frac{\partial \mathbf{n}}{\partial t}\right)\\
&= -\frac{1}{R_\alpha}\left(\frac{\partial}{\partial \xi_\alpha}\left(\mathbf{t}_\alpha\cdot\frac{\partial \mathbf{n}}{\partial t}\right) - \frac{1}{R_\alpha}\mathbf{n}\cdot\frac{\partial \mathbf{n}}{\partial t}\right)\\
&= -\frac{1}{R_\alpha}\frac{\partial}{\partial \xi_\alpha}\left(\mathbf{t}_\alpha\cdot\frac{\partial \mathbf{n}}{\partial t}\right)
\end{aligned} \tag{D.9a}$$

Switching the two scalar products of Eq. (D.8) by their simplified expressions (D.9b), it comes:

$$\frac{\partial R_\alpha}{\partial t} = -v + R_\alpha^2\frac{\partial}{\partial \xi_\alpha}\left(\mathbf{t}_\alpha\cdot\frac{\partial \mathbf{n}}{\partial t}\right) \tag{D.10}$$

The spatial derivative of (D.2) along t_α yields:

$$\frac{\partial \mathbf{v}}{\partial \xi_\alpha} = \frac{\partial^2 \mathbf{x}}{\partial \xi_\alpha \partial t} = \frac{\partial^2 \mathbf{x}}{\partial t \partial \xi_\alpha} = \frac{\partial \mathbf{t}_\alpha}{\partial t} \tag{D.11}$$

Seeing that (D.3) implies

$$\frac{\partial \mathbf{v}}{\partial \xi_\alpha} = \frac{\partial v\mathbf{n}}{\partial \xi_\alpha} = \frac{\partial v}{\partial \xi_\alpha}\mathbf{n} + v\frac{\partial \mathbf{n}}{\partial \xi_\alpha}, \tag{D.12}$$

the scalar product of (D.11) by $\mathbf{n}$ yields:

$$\frac{\partial v}{\partial \xi_\alpha} = \frac{\partial \mathbf{t}_\alpha}{\partial t}\cdot\mathbf{n} \tag{D.13}$$

Noting that $\mathbf{t}_\alpha\cdot\mathbf{n} = 0$ implies

$$\frac{\partial \mathbf{t}_\alpha}{\partial t}\cdot\mathbf{n} = -\frac{\partial \mathbf{n}}{\partial t}\cdot\mathbf{t}_\alpha \tag{D.14}$$

one gets

$$\frac{\partial \mathbf{n}}{\partial t}\cdot\mathbf{t}_\alpha = -\frac{\partial v}{\partial \xi_\alpha} \tag{D.15}$$

Using this last relation (D.15) in (D.10), we obtain:

$$\frac{\partial R_\alpha}{\partial t} = -v - R_\alpha^2\frac{\partial^2 v}{\partial \xi_\alpha^2} \tag{D.16}$$

Let $\mathbf{v}_{\tilde{\sigma}}$ be the velocity of the local coordinate $(\mathbf{g}_1, \mathbf{g}_2, \mathbf{g}_3)$ and D/Dt the real Lagrangian derivative, we have:

$$\frac{DR_\alpha}{Dt} = \frac{\partial R_\alpha}{\partial t} + \mathbf{v}_{\tilde{\sigma}}\cdot\mathbf{t}_\alpha\frac{\partial R_\alpha}{\partial \xi_\alpha}$$

After some algebra, we obtain:

$$\frac{DR_\alpha}{Dt} = -R_\alpha^2\frac{\partial^2 \mathbf{v}_{\tilde{\sigma}}}{\partial \xi_\alpha^2}\cdot\mathbf{n} + 2R_\alpha\frac{\partial \mathbf{v}_{\tilde{\sigma}}}{\partial \xi_\alpha}\cdot\mathbf{t}_\alpha \tag{D.17}$$

Noting κ the mean curvature,

$$\kappa = \kappa_1 + \kappa_2 = \frac{1}{R_1} + \frac{1}{R_2} \tag{D.18}$$

we finally find:

$$\frac{D\kappa}{Dt} = \Delta_s \mathbf{v}_{\tilde{\sigma}}\cdot\mathbf{n} - 2\nabla_s \mathbf{v}_{\tilde{\sigma}} : \mathbf{B} \tag{D.19}$$

References

Anderson, D.M., McFadden, G.B., Wheeler, A.A., 2001. A phase-field model with convection: sharp-interface asymptotics. Phys. D 151, 305–331.

Aris, R., 1962. Vectors, Tensors, and the Basic Equations of Fluid Mechanics. Dover, New York.

Bardina, J., Ferziger, J.H., Reynolds, W.C., 1983. Improved turbulence models for large eddy simulation. In AIAA Paper 83-1357.

Boivin, M., Simonin, O., Squires, K.D., 2000. On the prediction of gas–solid flows with two-way coupling using large eddy simulation. Phys. Fluids 12 (8), 2080–2090.

Calmet, I., Magnaudet, J., 2003. Statistical structure of high-Reynolds-number turbulence close to the free surface of an open-channel flow. J. Fluid Mech. 474, 355–378.

Chandesris, M., Jamet, D., 2006. Boundary conditions at a planar fluid-porous interface for a Poiseuille flow. Int. J. Heat Mass Transfer 49, 2137–2150.

Chandesris, M., Jamet, D., 2007. Boundary conditions at a fluid-porous interface: an a priori estimation of the stress jump coefficients. Int. J. Heat Mass Transfer 50 (17-18), 3422–3436.

Christensen, E.D., Deigaard, R., 2001. Large eddy simulation of breaking waves. Coastal Eng. 42, 53–86.

Delhaye, J.M., 1974. Jump conditions and entropy sources in two-phase systems. Local instant formulation. Int. J. Multiphase Flow 1, 395–409.

Drew, D.A., Lahey, R.T., 1987. The virtual mass and lift force on a sphere in rotating and straining inviscid flow. Int. J. Multiphase Flow 13, 113–121.

Drew, D.A., Passman, S.L., 1999. Theory of Multicomponent Fluids. Springer-Verlag, New York.

Van Dyke, M., 1975. Perturbation Methods in Fluid Mechanics. The Parabolic Press, Standford, California.

Eaton, J.K., Fessler, J.R., 1994. Preferencial concentration of particles by turbulence. Int. J. Multiphase Flow 16 (1), 169–209.

Edwards, D.A., Brenner, H., Wasan, D.T., 1991. Interfacial Transport Processes and Rheology. Butterworth-Heinemann.

Elghobashi, S., Abou-Arab, T., Rizk, M., Mostafa, A., 1984. Prediction of the particle-laden jet with a two-equation turbulence model. Int. J. Multiphase Flow 10 (6), 687–710.

Emmerich, H., 2003. The Diffuse Interface Approach in Materials Science. Springer.

Fouillet, C., 2003. Généralisation à des mélanges binaires de la méthode du second gradient et application à la simulation numérique directe de l'ébullition nucléée. Ph.D Thesis, vol. 6, Paris.
Garrigues, J., 1999. Statique des coques élastiques. <http://jgarrigues.perso.egim-mrs.fr/coques.html>.
Garrigues, J., 2001. Eléments d'algèbre et d'analyse tensorielle à l'usage des mécaniciens. <http://jgarrigues.perso.egim-mrs.fr/tenseurs.html>.
Homescu, D., Panday, P.K., 1999. Forced convection condensation on a horizontal tube: influence of turbulence in the vapor and liquid phases. J. Heat Transfer 174, 874–885.
Ishii, M., 1975. Thermo-fluid Dynamics Theory of Two-phase Flow. Eyrolles.
Labourasse, E., Lacanette, D., Toutant, A., Lubin, P., Vincent, S., Lebaigue, O., Caltagirone, J.P., Sagaut, P., 2007. Towards Large Eddy Simulation of isothermal two-phase flows: governing equations and a priori tests. Int. J. Multiphase Flow 33 (1), 1–39.
Lain, S., Bröder, D., Sommerfeld, M., Göz, M.F., 2002. Modelling hydrodynamics and turbulence in a bubble column using the Euler-Lagrange procedure. Int. J. Multiphase Flow 28 (8), 1381–1407.
Lakehal, D., Smith, B.L., Milelli, M., 2002. Large-eddy simulation of bubbly turbulent shear flows. J. Turbul. 3, 025.
Mathieu, B., 2003. Etude physique, expérimentale et numérique des mécanismes de base intervenant dans les écoulements diphasiques. PhD Thesis. University of Provence.
Menon, S., Yeung, P.K., Kim, W.W., 1996. Effect of subgrid models on the computed interscale energy transfer in isotropic turbulence. Comput. Fluids 25 (2), 165–180.
Sagaut, P., 2003. Large Eddy Simulation for Incompressible Flows. Springer-Verlag.
Sagaut, P., Germano, M., 2005. On the filtering paradigm for LES flow with discontinuities. J. Turbul. 6 (23), 1–9.
Sato, Y., Sekoguchi, K., 1975. Liquid velocity distribution in two-phase bubble flow. Int. J. Multiphase Flow 2, 79–95.
Shen, L., Yue, D.K.P., 2001. Large-eddy simulation of free surface turbulence. J. Fluid Mech. 440, 75–116.
Squires, K.D., Yamazaki, H., 1995. Preferential concentration of marine particles in isotropic turbulence. Deep Sea Res. Part I 42 (11–12), 1989–2004.
Toutant, A., Chandesris, M., Jamet, D., Lebaigue, O., accepted for publication. Jump conditions for filtered quantities at an under-resolved discontinuous interface. Part 2: a priori tests. Companion paper, Int. J. Multiphase Flow.
Toutant, A., Labourasse, E., Lebaigue, O., Simonin, O., 2006. Interaction between a deformable buoyant bubble and a homogeneous isotropic turbulence. In: Proceedings of Conference on Turbulence and Interaction, Porquerolles, France, 29 May–2 June.
Toutant, A., Labourasse, E., Lebaigue, O., Simonin, O., 2008. DNS of the interaction between a deformable buoyant bubble and a spatially decaying turbulence: a priori tests for LES two-phase flow modelling. Comput. Fluids 37 (7), 877–886.
Watanabe, Y., Saeki, H., 2002. Velocity field after wave breaking. Int. J. Numer. Meth. Fluids 39, 281–301.
Zeytounian, R.Kh., 1986. Les modèles asymptotiques de la mécanique des fluides I, Lecture Notes in Physics. Springer-Verlag, Berlin.
Zwillinger, D., 1989. Handbook of Differential Equations. Academic Press, Boston.